ISSN 1070-3284, Russian Journal of Coordination Chemistry, 2020, Vol. 46, No. 3, pp. 154–177. © Pleiades Publishing, Ltd., 2020.
Russian Text © The Author(s), 2020, published in Koordinatsionnaya Khimiya, 2020, Vol. 46, No. 3, pp. 132–156.

Complexes of Group III Metals Based on *o*-Iminoquinone Ligands

I. V. Ershova[a] and A. V. Piskunov[a, *]

[a] *Razuvaev Institute of Organometallic Chemistry, Russian Academy of Sciences, Nizhny Novgorod, 603950 Russia*
**e-mail: pial@iomc.ras.ru*

Received September 27, 2019; revised October 30, 2019; accepted October 31, 2019

Abstract—The currently available published data on the synthesis, structure, and chemical properties of Group III metal complexes based on bi-, tri-, and tetradentate *o*-iminoquinone redox-active ligands are presented and analyzed.

Keywords: *o*-iminobenzoquinone, redox-active ligands, Group III metals
DOI: 10.1134/S1070328420030021

INTRODUCTION

The chemistry of metal complexes with redox-active ligands has been intensively developed over the last several years owing to large diversity of practically useful properties inherent in compounds of this type owing to the organic moiety [1–6]. More and more unusual chemical transformations are becoming available because of the ability of the ligands to undergo reversible redox transformations within the metal coordination sphere [7–13]. Yet another important aspect of the chemistry of these compounds is the possibility of targeted design of magnetically active metal derivatives with radical forms of redox-active ligands. These properties are especially significant for the chemistry of Main Group metals, which are unable to easily change their oxidation states and do not tend to form paramagnetic stable ions. A recent publication is devoted to the coordination chemistry of Main Group IV metals with redox-active o-iminoquinone ligands [14]. This review summarizes published data on the synthesis, structure, and chemical properties of complexes of Group III elements, including rare earth elements and actinides, with ligands of this type.

GROUP III METAL COMPLEXES WITH BIDENTATE *o*-IMINOQUINONE LIGANDS

In the metal coordination sphere, bidentate ON-chelating redox-active *o*-iminobenzoquinone ligands can exist in any of three redox forms: neutral (*o*-iminobenzoquinone, imQ^0), singly reduced (*o*-iminobenzosemiquinolate, $imSQ^-$), and double reduced (*o*-amidophenolate, AP^{2-}) ones (Scheme 1).

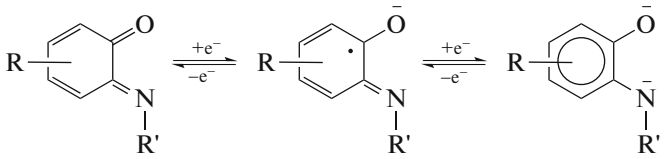

imQ imSQ AP

Scheme 1.

The key methods for the synthesis of Group III *o*-iminobenzoquinone metal complexes are generally similar and include direct reaction of metals (or their amalgams) with *o*-iminobenzoquinones, exchange reactions between the appropriate alkali metal derivatives and group III metal halides, and oxidative addition of *o*-iminobenzoquinones to metal compounds in low oxidation states. In the vast majority of synthetic approaches to the preparation of Al, Ga, In, and Tl *o*-iminobenzoquinone derivatives, sterically hindered 4,6-di-*tert*-butyl-*N*-(2,6-di-isopropylphenyl)-*o*-iminobenzoquinone (^{Dipp}imQ) and its mono- ((^{Dipp}imSQ)Na) and disodium ((^{Dipp}AP)Na_2) salts serve the starting compounds (Scheme 2).

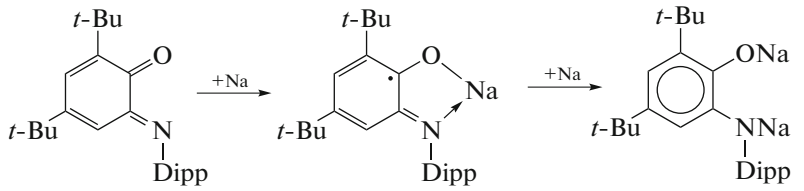

^{Dipp}imQ (^{Dipp}imSQ)Na (^{Dipp}AP)Na

Dipp = 2,6-di-isopropylphenyl

Scheme 2.

In some cases, where desired *o*-iminobenzoquinones are unstable in solution, the corresponding *o*-aminophenols (doubly reduced protonated *o*-iminobenzoquinone $(AP^{2-})H_2$) are used as the starting compounds for the synthesis of *o*-iminobenzoquinone metal derivatives.

Complexes of boron group elements. Since the chemistry of boron considerably differs from the chemistry of other Group III elements, none of the above-mentioned general methods is applicable for the preparation of its *o*-iminoquinone derivatives. Most of known boron *o*-amidophenolates are synthesized from *o*-aminophenols and boric acid derivatives [15, 16].

The reaction of two equivalents of phenylboronic acid and bis-*o*-aminophenols occurs under rather drastic conditions and gives bis-oxazaborolidines **1** containing two planar five-membered CCNBO rings in which each boron atom has a trigonal geometry (Scheme 3) [16]. Thus, despite the fact that formally tetradentate ONNO ligands were used as the starting compounds, complexes **1** represent two alkyl-bridged *o*-amidophenolate moieties (AP)BPh. In solution, all compounds of type **1** are symmetrical because of the presence of C_2 rotation axis; however, in the crystals, this symmetry is broken. The presence of two Lewis acid sites in one molecule makes compounds **1** of interest for bimolecular catalysis.

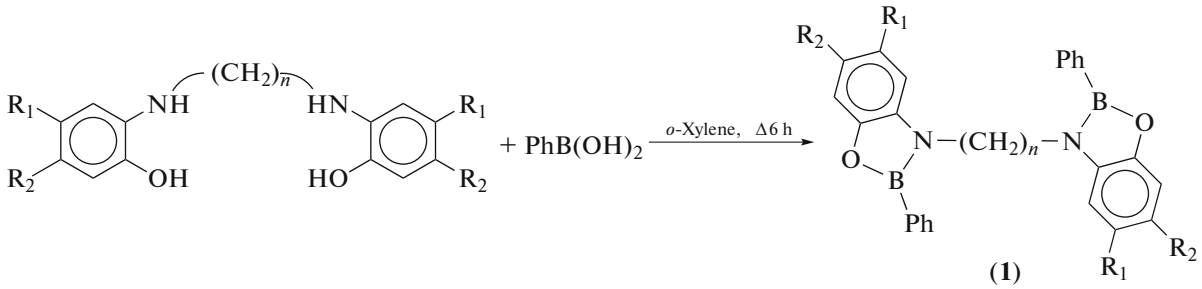

(**1**)

R_1, R_2 = H, Me, *t*-Bu; *n* = 2, 3

Scheme 3.

A complex of different type containing two (AP)B moieties in one molecule was obtained in a moderate yield upon the reaction of unsubstituted *o*-aminophenol with the diborane $B_2(NMe_2)_4$ (Scheme 4) [17]. Dimeric complex **2** is located at the inversion center: the O atoms and NH groups of two (AP)B molecules are in *trans*-positions relative to each other. According to X-ray diffraction data, π-stacking with interplanar spacing of 3.48 Å is present in the crystal of **2**. In addition, each molecule of **2** is connected to four other molecules of two neighboring columns through NH···O contacts (2.32 Å), thus forming infinite sheets of hydrogen-bonded molecules.

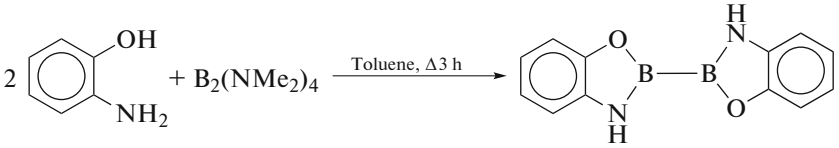

(**2**)

Scheme 4.

Boron-containing ferrocenyl complexes **3**, which are formed upon the reaction of boric acid derivatives with *o*-aminophenol functionalized with a bis(diphenylphosphine)ferrocenyl group (Scheme 5), are promising ligands for asymmetric catalysis due to secondary interactions between the boronate group, which is a weak Lewis acid site, and the substrate, which is a Lewis base [15]. Complexes **3** form stable metal complexes **4** when treated with $Me_2Pt(COD)$ (COD is cyclooctadiene) (Scheme 5) and stable adducts with Rh(I) complexes, exhibiting catalytic activity towards hydrogenation and hydroformylation of simple substrates.

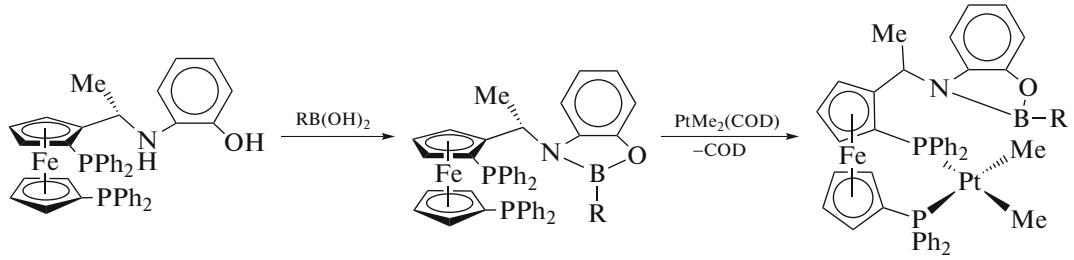

(3) **(4)**

R = Me, Ph, *p*-C_6H_4Cl

Scheme 5.

Meanwhile, when unsubstituted *o*-aminophenol reacts with Me_3Ga, only the hydroxyl group of the ligand is deprotonated and *o*-aminophenolate rather than *o*-amidophenolate complex is formed as the reaction product (Scheme 6) [18]. Analysis of the crystal structure of **5** showed that molecules of the complex do not form dimers, but are bound to neighboring molecules by NH···O hydrogen bonds.

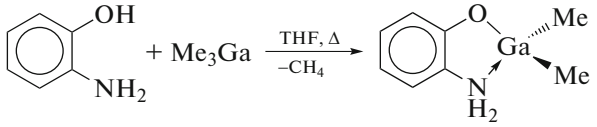

(5)

Scheme 6.

Gallium metal does not react with ^{Dipp}imQ; however, the reaction of gallium amalgam involves incomplete reduction of ^{Dipp}imQ to give mixed-ligand complex **6** (Scheme 7) [19]. The presence of two differently charged *o*-iminoquinone ligands in **6** is unambiguously indicated by ESR spectroscopy data, pointing to the presence of fast (on the ESR time scale) migration of the unpaired electron between two redox-active ligands. Decoordination of the THF molecule upon dissolution of **6** in hexane leads to a change in the geometry of the resulting four-coordinate complex **7** to a tetrahedral geometry in which delocalization of the unpaired electron over both ligands is impossible. Complex **8** formed upon the addition of pyridine to a solution of **7** was isolated in a pure state. The structure of this complex in solution is similar to that of **6** and is retained in the crystalline state, as indicated by the presence of ligand–ligand charge transfer band (~2010 nm) in the near IR range.

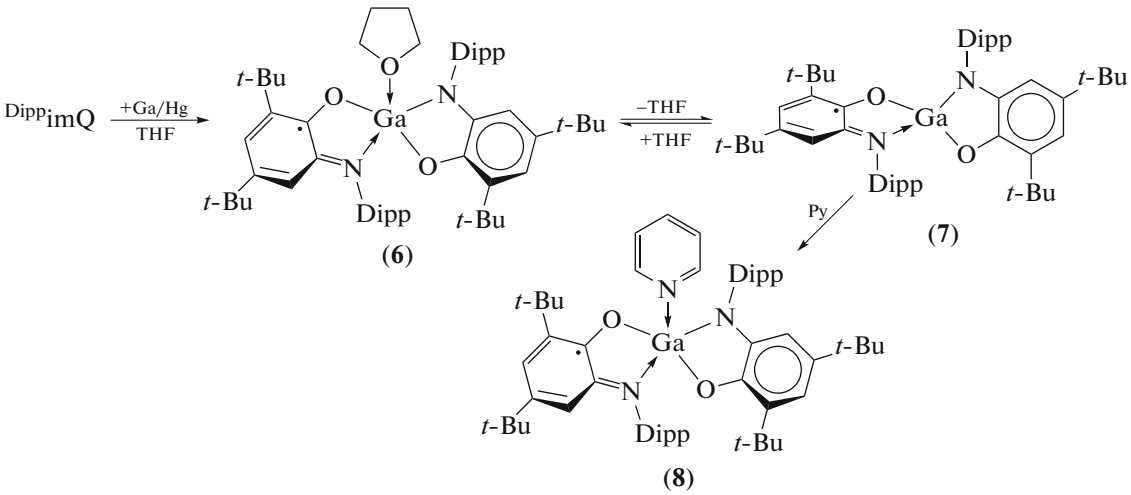

(6) **(7)** **(8)**

Scheme 7.

A convenient method for the synthesis of metal complexes containing a redox-active ligand as the dianion is reduction of *o*-iminoquinone with metal halides in low oxidation states. The reaction of ^{Dipp}imQ with "GaI" affords *o*-amidophenolate **9**, which can also be synthesized by the reaction of ^{Dipp}imQ with gallium metal in the presence of a stoichiometric amount of iodine (Scheme 8) [19].

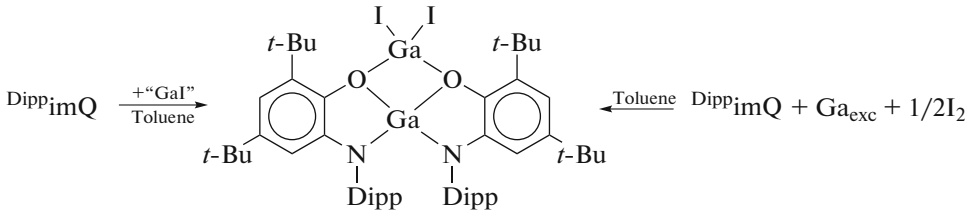

[(^{Dipp}AP)GaI]$_2$ (**9**)

Scheme 8.

When (^{Dipp}AP)Na$_2$ is used as the starting compound, gallium *o*-amidophenolate derivatives are formed by exchange reaction with metal halides: dimeric gallium *o*-amidophenolate **10** is obtained by reaction between (^{Dipp}AP)Na$_2$ and MeGaI$_2$ (Scheme 9) [20], whereas the formation of either **11** [21] or **12** [19] in the reaction of (^{Dipp}AP)Na$_2$ with GaI$_3$ depends on the reactant ratio (2 : 1 or 3 : 2, respectively) (Scheme 10).

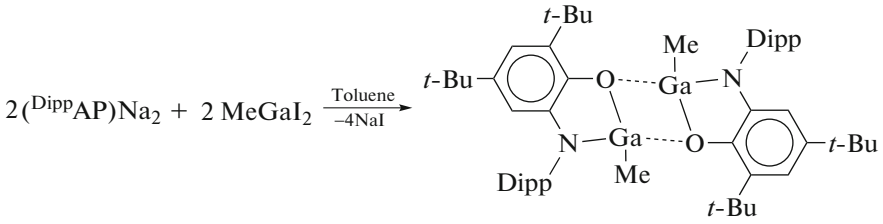

[(^{Dipp}AP)GaMe]$_2$ (**10**)

Scheme 9.

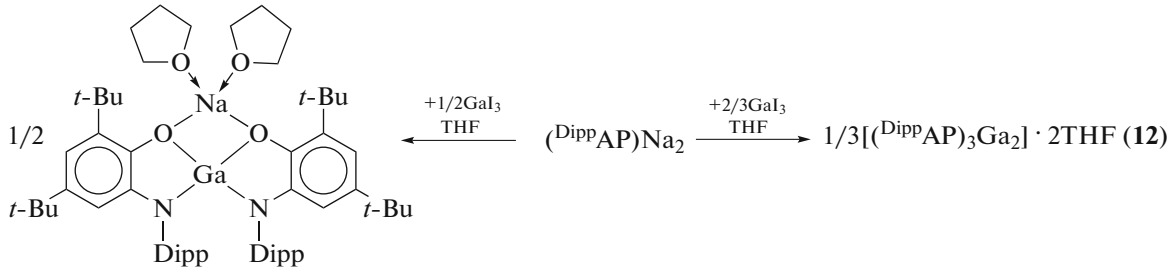

[(^{Dipp}AP)$_2$GaNa] · 2THF (**11**)

Scheme 10.

The reactions of ^{Dipp}imQ with low-oxidation-state indium iodides does not result in the formation of *o*-amidophenolate derivatives: the reaction between ^{Dipp}imQ and InI gives biradical complex **13**, while In_2I_4 disproportionates in the presence of ^{Dipp}imQ and thus a mixture of products **13** and **14** is formed (Scheme 11) [22]. Complex **14** containing metal-coordinated ^{Dipp}imQ ligand can also be obtained by direct reaction of ^{Dipp}imQ with InI_3 in toluene.

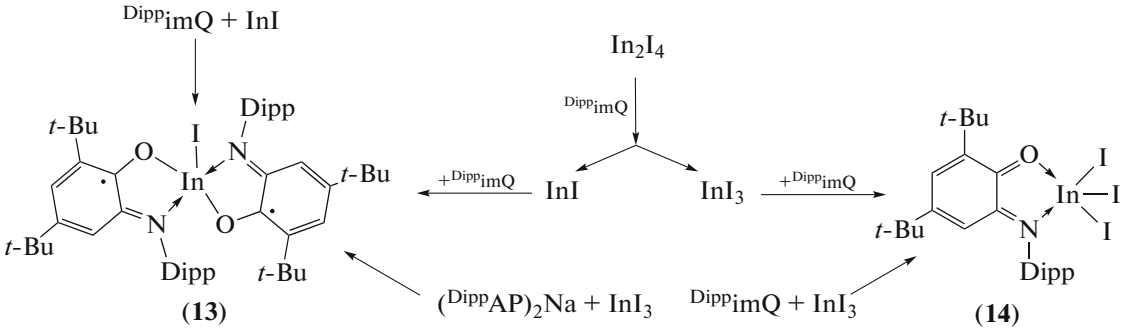

Scheme 11.

The reaction of $(^{Dipp}AP)Na_2$ with InI_3 in non-polar solvents is accompanied by oxidation of the *o*-amidophenolate ligand with the In^{3+} ion, and paramagnetic complex **13** is again formed (Scheme 11). The redox process between $(^{Dipp}AP)^{2-}$ and In^{3+} was suppressed in [23] by using the strategy of decreasing the electron-acceptor properties of In^{3+} by introduction of a neutral N-donor ligand into the metal coordination sphere and by replacement of the electron-withdrawing iodine atom by an electron-donating alkyl group; this furnished indium *o*-amidophenolates **15** and **16** (Scheme 12).

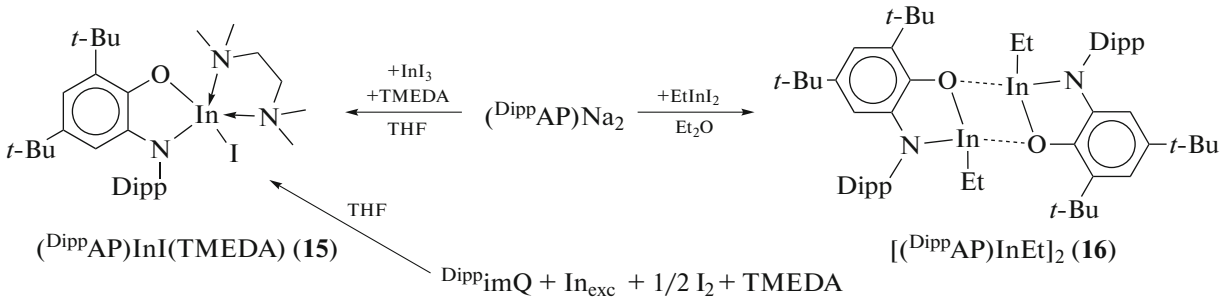

Scheme 12.

Indium bis-*o*-amidophenolate obtained by exchange reaction between $(^{Dipp}AP)Na_2$ and InI_3 (2 : 1) in THF represents ionic complex $[(^{Dipp}AP)_2In]^-[Na(DME)_3]^+$ **17**, unlike gallium analogue **11** (Scheme 13) [24]. Complex **17** is also formed via the reduction of the $(^{Dipp}imSQ)^-$ radical anion by monovalent indium ion (Scheme 13).

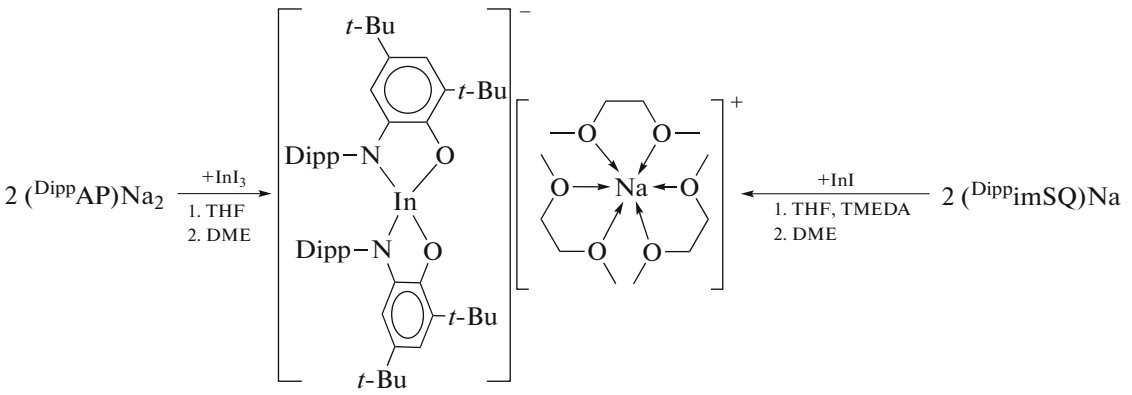

$[(^{Dipp}AP)_2In]^-[Na(DME)_3]^+$ (**17**)

Scheme 13.

The reaction of gallium (**11**) or indium (**17**) bis-*o*-amidophenolate with excess alkyl/allyl halides (RHal) involves the oxidative addition of two RHal molecules to Main Group metal complexes accompanied by the formation of two new C–C bonds [21, 24]. The reactions proceed under relatively mild conditions and afford diamagnetic complexes **18**, which contain iminocyclohexa-1,4-dienolate type ligands (Scheme 14).

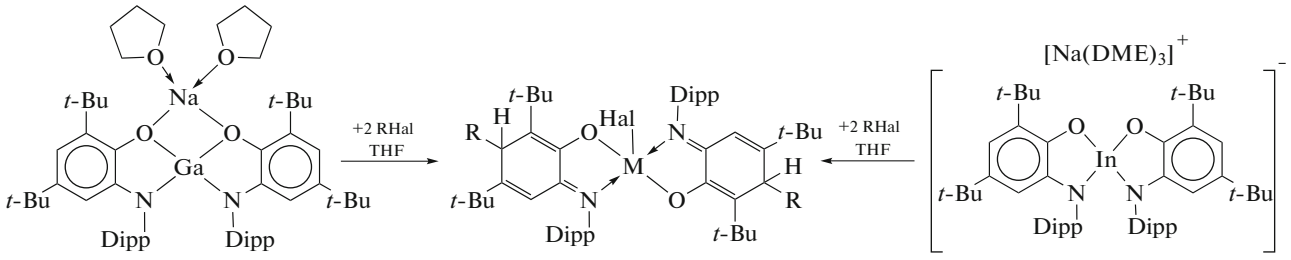

[(^{Dipp}AP)$_2$Ga]Na · 2THF (**11**) $^{R}L_2MHal$ (**18**) [(^{Dipp}AP)$_2$In]$^-$[Na(DME)$_3$]$^+$ (**17**)

M = Ga, R = All; Hal = Cl, Br, I

M = In, R = Me, Et; Hal = I

Scheme 14.

The reactions of gallium *o*-amidophenolate complexes **9** and **10** with single-electron oxidants are accompanied by oxidation of the (^{Dipp}AP)$^{2-}$ ligand of the starting compounds, giving rise to new paramagnetic gallium derivatives (Scheme 15) [25]. The first steps of these reactions involve the formation of monoradical intermediates, detected by ESR spectroscopy, which subsequently undergo symmetrization to afford biradical metal complexes **19**–**22**. Complex **19** is also a major product of oxidation of **10** with oxygen [20].

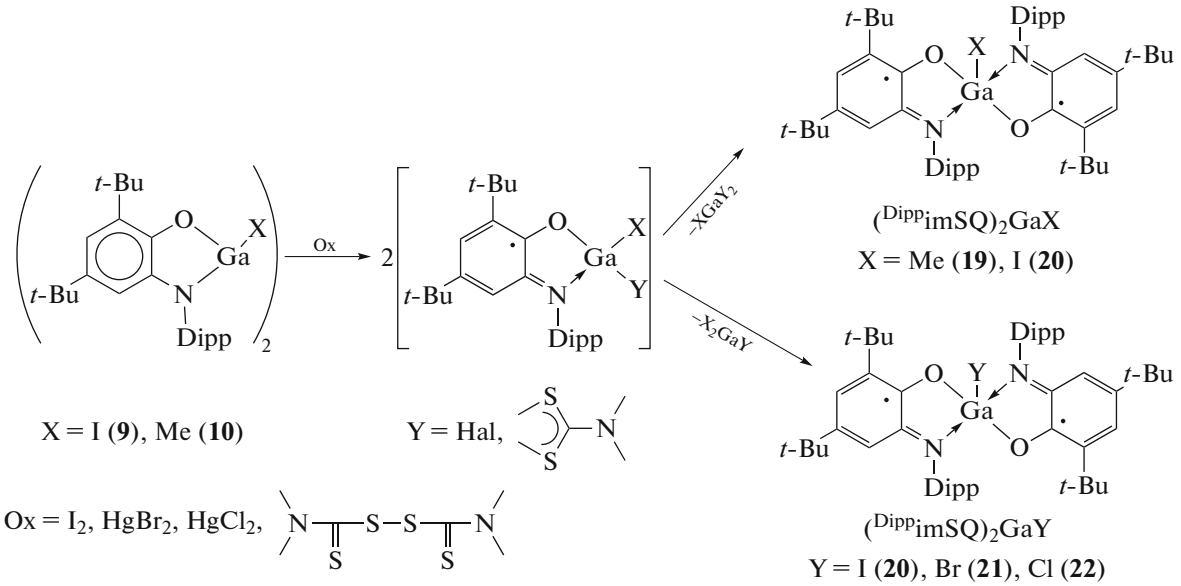

(^{Dipp}imSQ)$_2$GaX

X = Me (**19**), I (**20**)

X = I (**9**), Me (**10**)

Y = Hal,

Ox = I_2, $HgBr_2$, $HgCl_2$,

(^{Dipp}imSQ)$_2$GaY

Y = I (**20**), Br (**21**), Cl (**22**)

Scheme 15.

Indium *o*-amidophenolate [(^{Dipp}AP)InEt]$_2$ **16** is oxidized with single-electron oxidants or oxygen in a similar way. However, symmetrization of the intermediate monoradical complexes gives, in all cases, (^{Dipp}imSQ)$_2$InEt **23** [26]. The oxidation of (^{Dipp}AP)InI(TMEDA) (**15**) with oxygen also results in the formation of biradical complex (^{Dipp}imSQ)$_2$InI (**13**), whereas the reactions of **15** with I_2 and $HgCl_2$ also afford monoradical complexes **24** and **25** (Scheme 16) [26]. The stability of **24** and **25** is attributable to the coordination of neutral *N*-donor ligand to the metal center, which prevents their subsequent symmetrization [23].

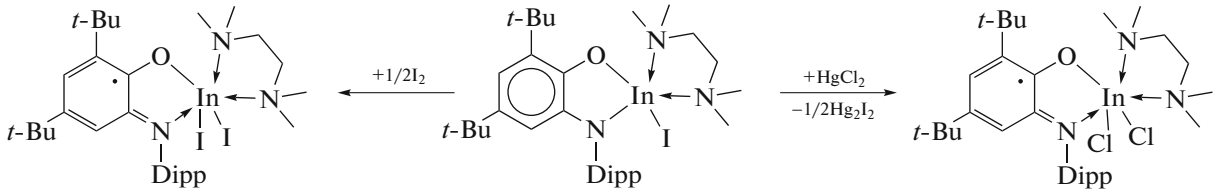

(**24**) (**15**) (**25**)

Scheme 16.

The symmetrization pathway of monoradical indium complexes is determined by the degree of filling of the metal coordination sphere in the products; therefore, the formation of six-coordinate complex **26** rather than five-coordinate **13** upon the oxidation of **15** with tetramethylthiuram disulfide is quite reasonable (Scheme 17) [26].

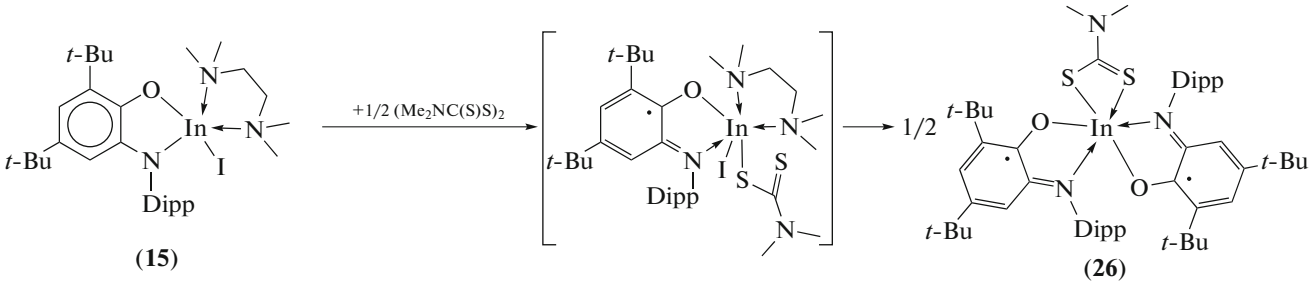

(**15**) (**26**)

Scheme 17.

The oxidation of indium bis-*o*-amidophenolate complex **17** with mercury(II) halides also results in the formation of bis-*o*-iminobenzosemiquinone derivatives **27** and **28** (Scheme 18) [27].

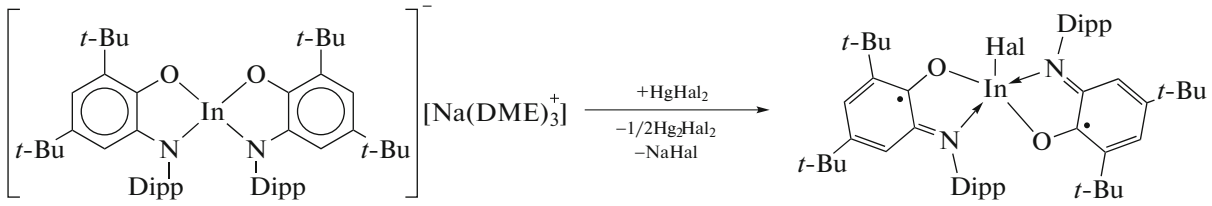

$[(^{Dipp}AP)_2In]^-[Na(DME)_3]^+$ (**17**)

$(^{Dipp}imSQ)_2InHal$ (Hal = Cl (**27**), Br (**28**))

Scheme 18.

The exchange reaction between $(^{Dipp}imSQ)Na$ and the corresponding metal halides/alkyl halides is the most convenient synthetic route to biradical derivatives of gallium [25, 28] and indium [22, 26]—final oxidation products of *o*-amidophenolate complexes **9**, **10**, and **16**—and biradical derivative of aluminum [29] (Scheme 19).

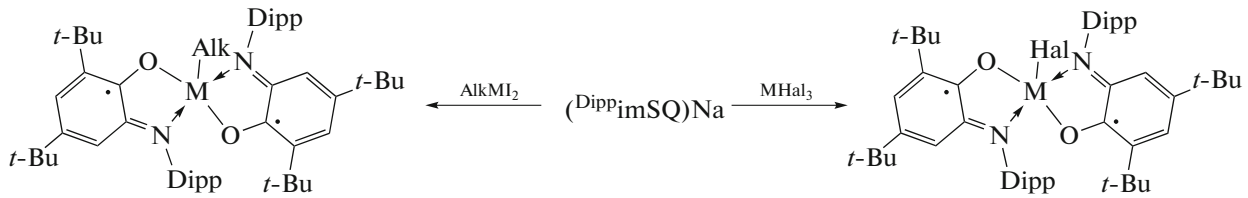

M = Ga, Alk = Me (**19**), Et (**29**)
M = In, Alk = Me (**30**), Et (**23**)

M = Ga, Hal = Cl (**22**), Br (**21**), I (**20**)
Hal = I, M = In (**13**), Al (**31**)

Scheme 19.

Using (^{Dipp}imSQ)$_2$MI (M = Al (**31**), Ga (**20**)) as the starting compounds, aluminum and gallium complexes **32**–**38** with various inorganic (and phenoxyl) substituents in the apical position were prepared by exchange reactions with excess inorganic salts (NaN_3, KNCS, KNCO) and stoichiometric amounts of sodium phenoxide (Scheme 20) [27–29].

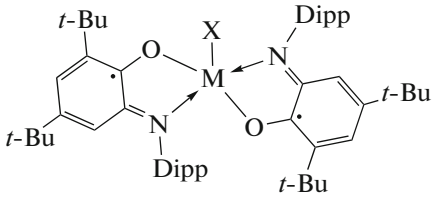

(^{Dipp}imSQ)$_2$MX

M = Al; X = N_3 (**32**), NCS (**33**), NCO (**34**)
M = Ga; X = N_3 (**35**), NCS (**36**), NCO (**37**), OPh (**38**)

Scheme 20.

The magnetic properties of a series of (^{Dipp}imSQ)$_2$MX complexes **13**, **19**–**23**, **27**–**38** depend substantially on the nature of the apical substituent X. In the complexes with alkyl substituents, weak ferromagnetic coupling takes place between the unpaired electrons of the radical anion ligands. In the case of derivatives with inorganic substituents and the complex with a phenoxyl group, rather strong antiferromagnetic exchange is present between the spins of the organic ligands. Density functional theory calculations performed for a series of (^{Dipp}imSQ)$_2$GaX complexes revealed indirect antiferromagnetic exchange via interaction of *p*-orbitals of the *o*-iminobenzoquinone oxygen and nitrogen atoms with the *p*- or π-orbitals of heteroatoms of the apical substituent X [28]. The magnetic exchange energy is correlated with the Ga–X bond length [27]. The coordination of the neutral donor ligands to the metal center (Scheme 21) changes the molecular geometry from five to six coordination and disrupts the indirect magnetic exchange [27].

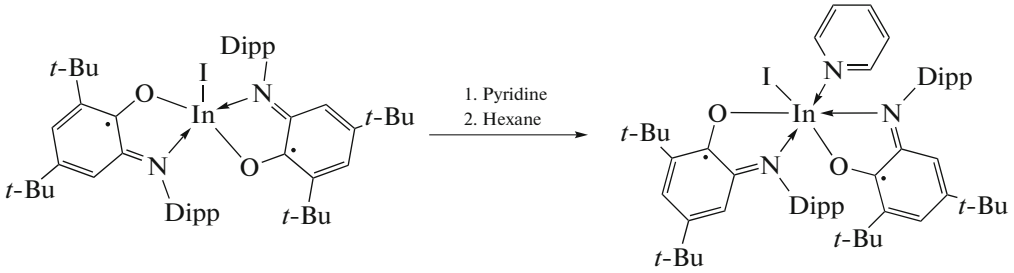

(^{Dipp}imSQ)$_2$InI (**13**) (^{Dipp}imSQ)$_2$In(I)Py (**39**)

Scheme 21.

Gallium tris-*o*-iminobenzosemiquinone complexes (imSQ^R)$_3$Ga (**40**) are formed upon the reactions of *o*-aminophenols with $GaCl_3$ in the presence of a base and air oxygen [30]. However, the absence of *ortho*-substituents relative to nitrogen in the *N*-aryl moiety may lead to instability of triradical compounds of this type and may be accompanied by intramolecular transformations of radical ligands, which was demonstrated for the complex with methoxy groups [31]. The reaction gave monoradical gallium complex **41** containing a hexadentate ligand, resulting from intramolecular rearrangement with C–H bond activation and formation of new C–N bonds (Scheme 22).

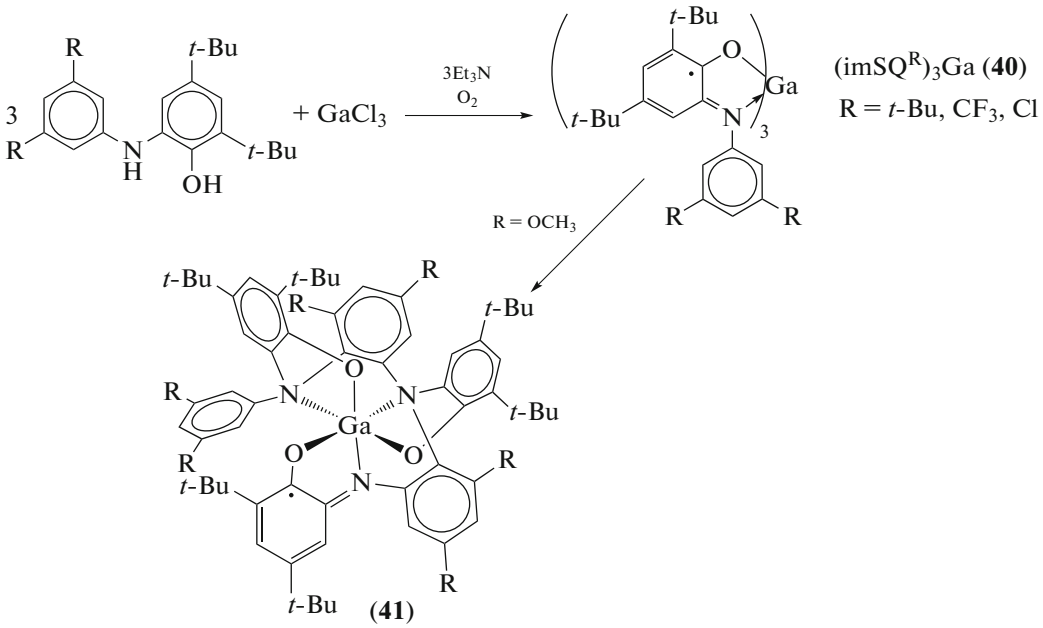

Scheme 22.

N-(2,6-Dimethylphenyl)phenanthrene-*o*-iminoquinone (^{Dmp}PhenimQ) is also used as a ligand for the synthesis of *o*-iminoquinone complexes. The reaction of an equimolar mixture of ^{Dmp}PhenimQ and $B(C_6F_5)_3$ in the presence of hydrogen in refluxing toluene for 1 h gives a mixture of diamagnetic (**42**) and paramagnetic (**43**) products, while the subsequent heating of the reaction mixture is accompanied by quantitative conversion of **42** to boron *o*-amidophenolate **44** (Scheme 23) [32]. Complex **43** is a rare example of structurally characterized polyaromatic borocyclic radical. Its stability under aerobic conditions is due to spin density delocalization over the aromatic skeleton of the redox-active ligand, which is confirmed by ESR data.

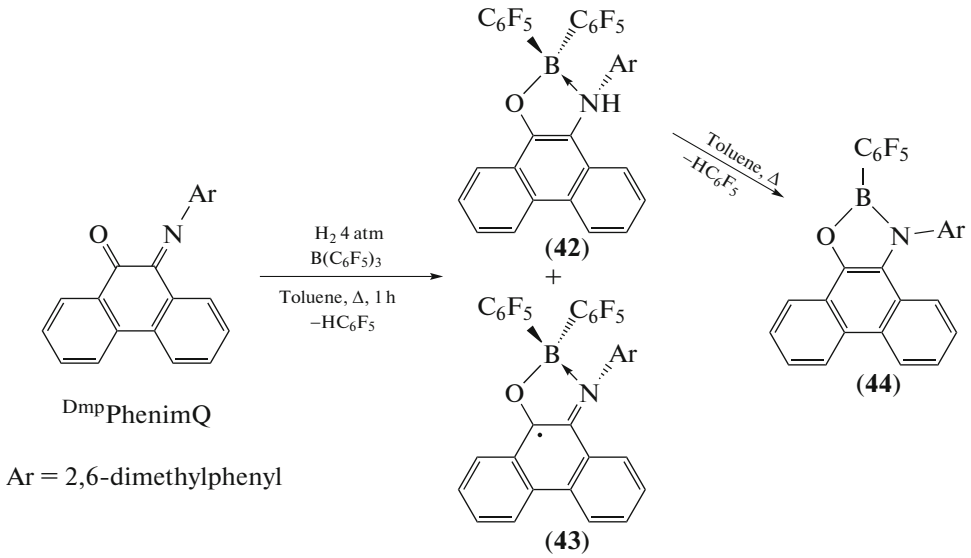

Scheme 23.

Since the synthesis shown in Scheme 23 results in the formation of a mixture of complexes **43** and **44** difficult to separate, alternative synthetic procedures were proposed for their synthesis, namely, the reaction of ^{Dmp}PhenimQ with $H_2B(C_6F_5) \cdot SMe_2$ (1 : 1) at room temperature for complex **44** and the reaction of ^{Dmp}PhenimQ with $HB(C_6F_5)_2$ for complex **43**.

Equimolar amounts of ^{Dmp}PhenimQ and Me_3Al react to afford diamagnetic binuclear complex **45**; this is accompanied by disruption of the conjugated structure of the ligand due to migration of one methyl group of $AlMe_3$ to the carbon atom bonded to the ligand oxygen atom, resulting in the C–C bond formation (Scheme 24) [33].

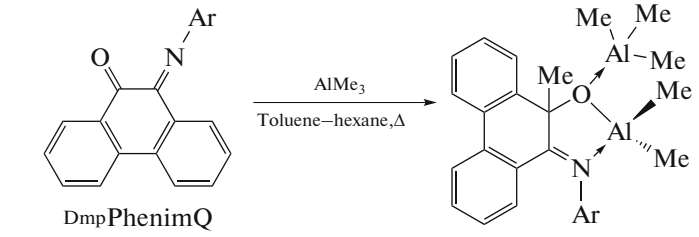

^{Dmp}PhenimQ (**45**)

Ar = 2,6-dimethylphenyl

Scheme 24.

Gallium complex containing a coordinated neutral *o*-iminoquinone ligand was obtained by the reaction of $GaCl_3$ with acenaphthene-1-imin-2-ones (^{Dipp}MIAN) (Scheme 25) [34]. The crystal cell of **46** contains single $[(^{Dipp}MIAN)_2GaCl_2]^+[GaCl_4]^-$ ions, presumably resulting from disproportionation of initially formed $(^{Dipp}MIAN)GaCl_3$.

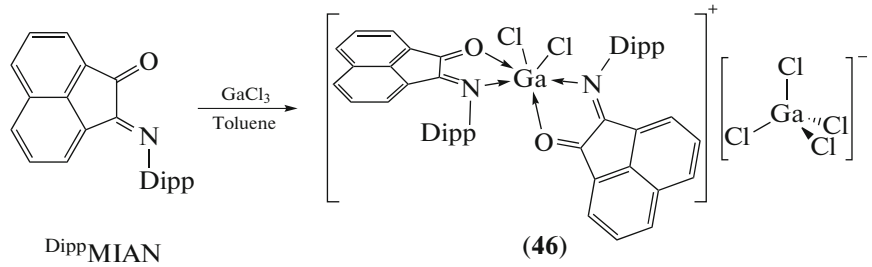

^{Dipp}MIAN (**46**)

Scheme 25.

Gallium complexes containing ^{Dipp}MIAN in singly and doubly reduced forms were prepared by stepwise reduction of the ligand with gallium metal in the presence of a stoichiometric amount of iodine (Scheme 26) [35]. Dimeric diamagnetic complex **48** reacts with phenylacetylene to give cycloaddition product **49**; also, compound **48** exhibits catalytic activity in hydroamination and hydroarylation of unsaturated substrates.

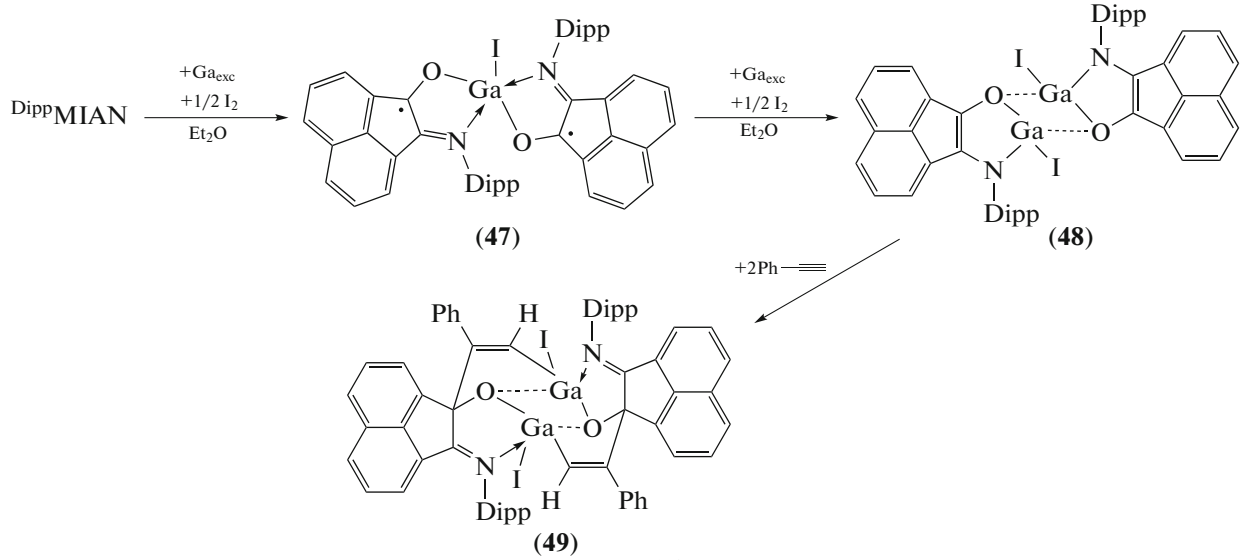

Scheme 26.

The only currently known thallium *o*-iminobenzoquinone derivative is thallium(I) *o*-iminobenzosemiquinolate (^{Dipp}imSQ)Tl (**50**), which is formed upon reduction of ^{Dipp}imQ with thallium amalgam [36].

Rare earth metal and actinide complexes. The first *o*-iminoquinone complexes of rare earth metals were obtained from *N*-(2,6-di-isopropylphenyl)phenanthrene-*o*-iminoquinone (^{Dipp}PhenimQ) [37]. The scandium and ytterbium oxidation with ^{Dipp}PhenimQ in benzene gives tris-ligand derivatives of trivalent metals **51** and **52** containing equivalent radical anion ligands ^{Dipp}PhenimSQ. However, according to NMR spectroscopy data, in THF, the obtained complexes occur in equilibrium with their *o*-amidophenolate forms (Scheme 27).

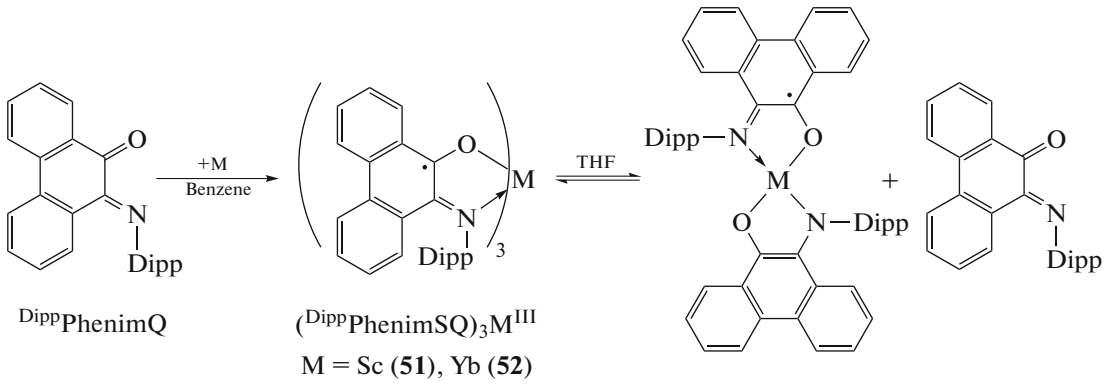

^{Dipp}PhenimQ — (^{Dipp}PhenimSQ)$_3$M^{III}, M = Sc (**51**), Yb (**52**)

Scheme 27.

The reactions of ^{Dipp}PhenimQ with neodymium(II) and dysprosium(II) iodides also lead to the formation of metal complexes formed by trivalent lanthanides, but, apart from two iodine atoms, the metal coordination spheres of **53** and **54** contain two differently charged redox-active ligands ^{Dipp}PhenimQ and ^{Dipp}PhenimSQ. Both ligands are coordinated to the metal according to the η^1 fashion, which is highly unusual for *o*-iminoquinones (Scheme 28). During the reaction, partial disproportionation of **53** and **54** takes place, giving rise to lanthanide triiodide and (^{Dipp}PhenimSQ)$_3$M; however, only the dysprosium complex (^{Dipp}PhenimSQ)$_3$Dy (**55**) (whose structure is similar to those of **51** and **52**) was isolated from the reaction mixture.

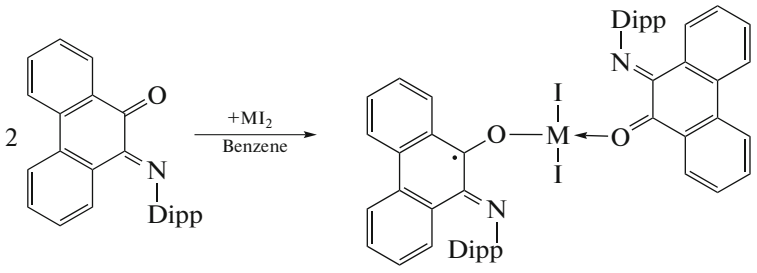

^{Dipp}PhenimQ — M = Nd (**53**), Dy (**54**)

Scheme 28.

The oxidation of ytterbium and europium with ^{Dipp}imQ affords complexes of divalent rather than trivalent lanthanides (**56** and **57**). The same products can also be prepared by the exchange reaction between (^{Dipp}AP)K$_2$ and the diiodides of the corresponding metals (Scheme 29) [38].

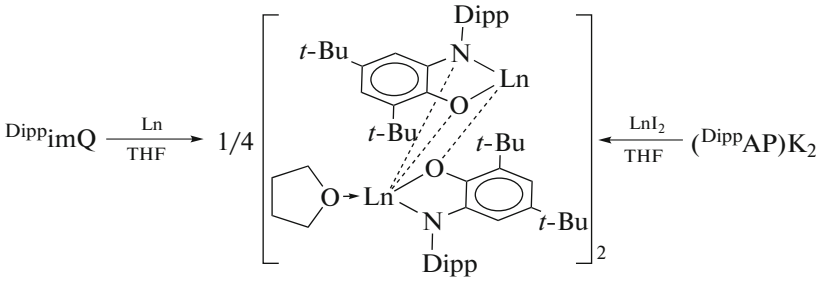

Ln = Yb (**56**), Eu (**57**)

Scheme 29.

The oxidative addition of an equivalent of ^{Dipp}imQ to *o*-amidophenolate Yb(II) (**56**) and Eu(II) (**57**) derivatives is accompanied by lanthanide oxidation to Ln(III) (Ln = Yb, Eu) and affords mixed-ligand derivatives **58** and **59**; alternatively, these complexes can be obtained by exchange reaction between (^{Dipp}imSQ)K and LnI_2 (2 : 1). When **56** is oxidized in a non-coordinating solvent, *o*-amidophenolate-bridged dimer **60** is formed (Scheme 30).

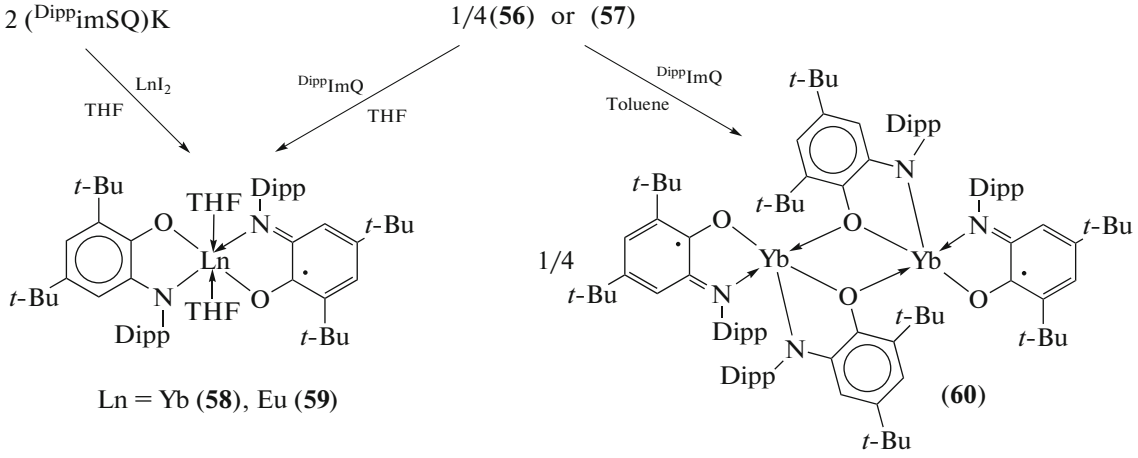

Scheme 30.

A series of ^{Dipp}imQ-based neodymium(III) bis-*o*-iminoquinone complexes was prepared, with the ^{Dipp}imQ ligand existing in three different redox states [39]. The complex (^{Dipp}imQ)$_2$NdI$_3$ (**61**) containing coordinated neutral *o*-iminoquinone ligands was prepared by the reaction of two equivalents of ^{Dipp}imQ with $NdI_3 \cdot 3.5THF$. The successive reduction of ^{Dipp}imQ within the coordination sphere of **61** with KC_8 furnishes bis-*o*-iminobenzosemiquinone (**62**) and bis-*o*-amidophenolate (**63**) Nd(III) derivatives. Complex **64**, produced upon treatment of **63** with crown ether, does not have a potassium cation in the neodymium coordination sphere (Scheme 31).

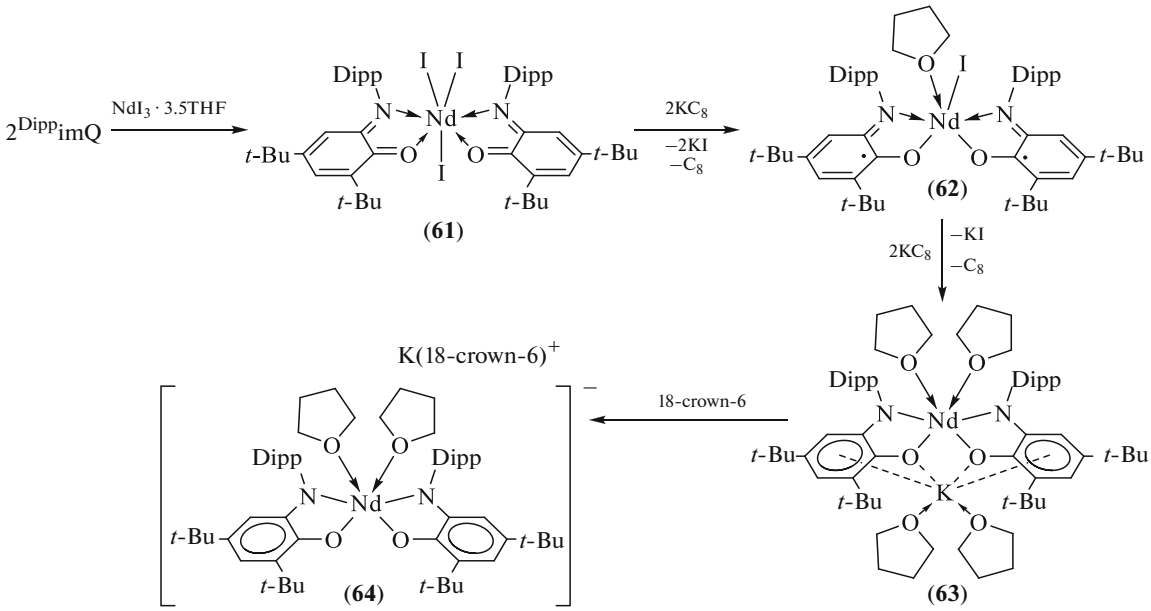

Scheme 31.

Complex **64** is rapidly oxidized with elemental sulfur and selenium to give bis-*o*-iminobenzosemiquinone complexes **65** and **66**, respectively, in which neodymium-coordinated chalcogen atoms form six-membered rings (Scheme 32). These reactions attract particular attention, because of the fact that participation in multielectron processes is highly unusual for lanthanides. Complex **63** also reacts with sulfur to give **65**, but does not react with selenium because the metal center is blocked by the potassium ion; however, when crown ether is added to the reaction mixture, compound **66** is rapidly formed.

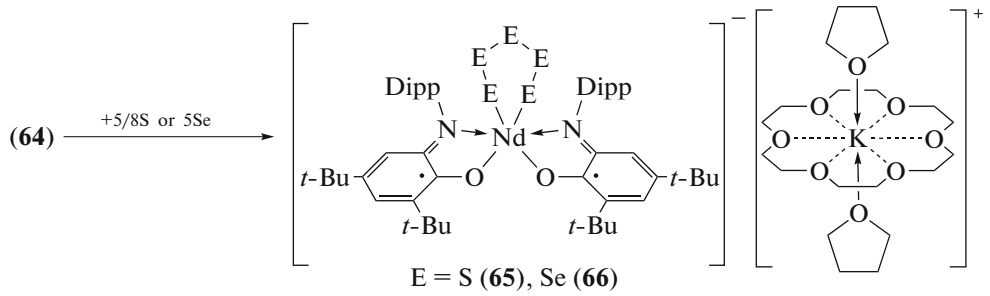

Scheme 32.

Complexes of actinides with *o*-iminoquinone ligands are represented by uranium and thorium compounds. Uranium(IV) complex **67** containing *o*-amidophenolate ligand ^{Dipp}AP is prepared from tetrabenzyluranium via successive reductive elimination of the benzyl radicals under the action of ^{Dipp}imQ [40]. The formation of *o*-iminosemiquinone intermediate **68** in the first stage of the reaction was proved by conducting the experiment with $U(CD_2C_6D_5)$; however, attempted synthesis of **68** resulted in complex **67** being isolated from the reaction mixture (Scheme 33). The targeted synthesis of **68** was performed from (^{Dipp}imSQ)$UI_3(THF)_2$ (**69**), which was prepared by oxidative addition of ^{Dipp}imQ to uranium(III) iodide. Treatment of **69** with KC_8 led to reduction of (^{Dipp}imSQ) to give uranium(IV) *o*-amidophenolate (^{Dipp}AP)$UI_2(THF)_2$ (**70**). The exchange reaction of **70** with one equivalent of $PhCH_2K$ was accompanied by the formation of the monoalkyl complex (^{Dipp}AP)$UI(CH_2Ph)(THF)_2$ (**71**), whereas attempted synthesis of **67** by exchange reaction of **70** with two equivalents of $PhCH_2K$ resulted in decomposition of the product.

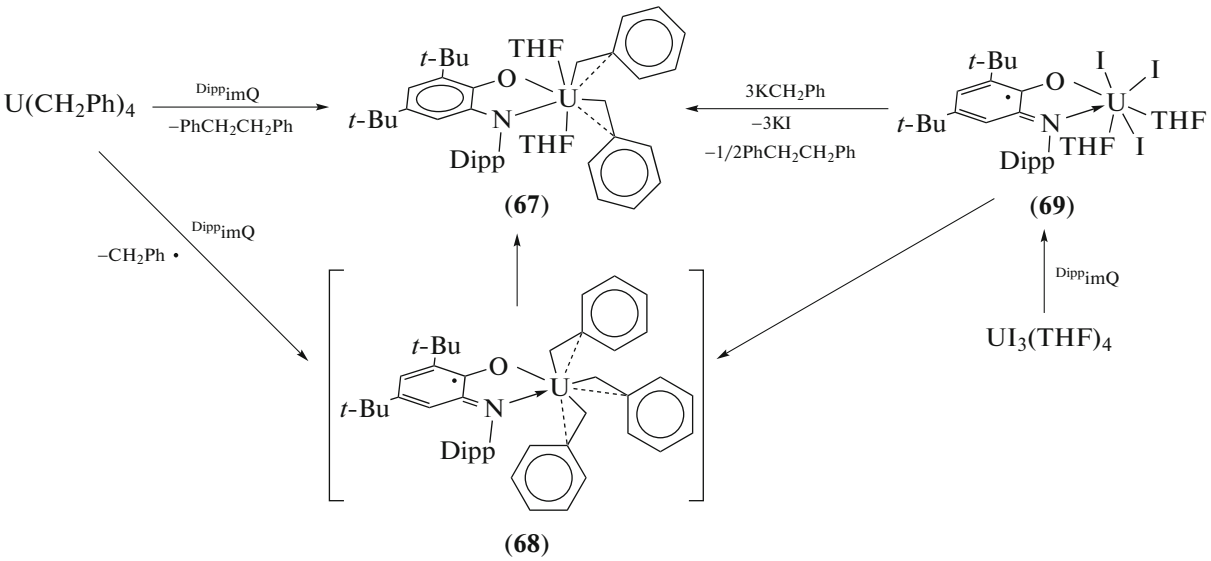

Scheme 33.

The exchange reaction between alkali metal *N*-*tert*-butyl-, *N*-adamantyl-, and *N*-dipp-substituted *o*-amidophenolates and uranium tetrachloride in 2 : 1 ratio gives rise to uranium(IV) bis-*o*-amidophenolate complexes **72**–**74** (Scheme 34) [41].

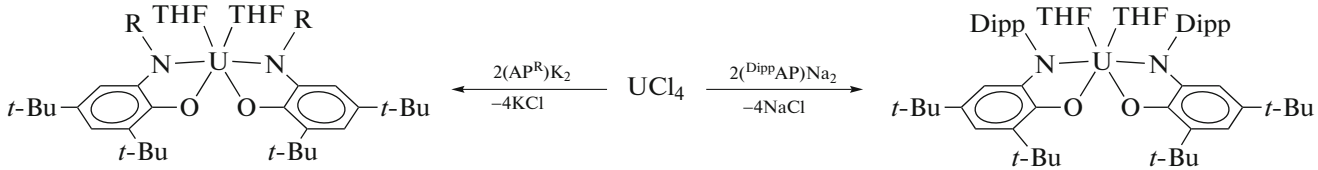

Scheme 34.

On treatment of complexes **72**–**74** with an equivalent of iodobenzene dichloride, oxidative addition of chlorine to the complexes takes place, resulting in the formation of bis-*o*-iminosemiquinone derivatives **75**–**77** (Scheme 35). The bis-*o*-iminosemiquinone complex $(imSQ^{t\text{-}Bu})_2UI_2(THF)$ (**78**) is the product of oxidative addition of iodine to complex **72**, whereas complexes **73** and **74** decompose on treatment with iodine.

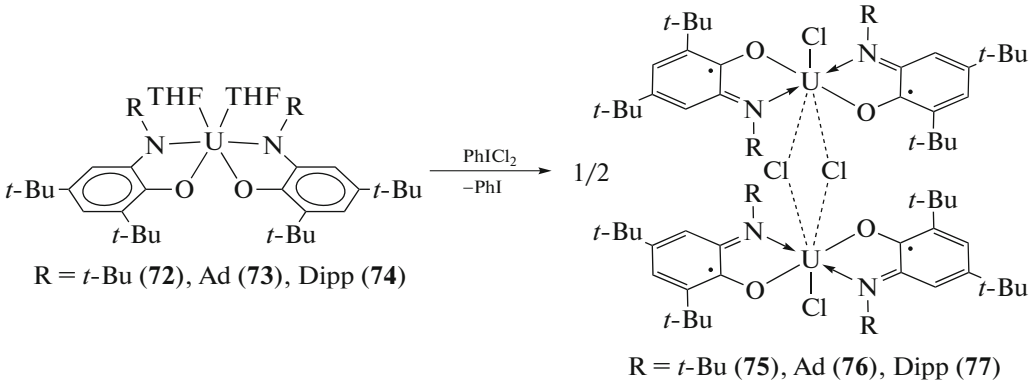

Scheme 35.

The first binuclear complexes of actinides with quinone-bridged metal centers were obtained by the reactions of 2,5-bis[2,6-di-isopropyl)anilide]-1,4-benzoquinone and 2,5-bis[2-(methoxy)anilide]-1,4-benzoquinone dianions with uranium(IV) and thorium(IV) complexes based on tripodal tris[2-amido(2-pyridyl)ethyl]amine (L) (Scheme 36) [42]. The presence of ligand L in the actinide coordination sphere

accounts for the kinetic and thermodynamic stability of binuclear complexes **79**–**81**. Thorium complexes **79** and **80** are diamagnetic, whereas **81** has two U(IV) magnetic centers. However, according to magnetochemical data, the magnetic exchange coupling between them is negligibly small. The reduced form of **81**, $[K(18\text{-c-}6)(THF)_2]^+[81^-]$, is unstable and highly sensitive to air oxygen and moisture. However, according to X-ray diffraction data, it is a new type of $U^{IV}U^{IV}$ complex in which the metal centers are linked by the *para*-iminoquinone radical anion bridge.

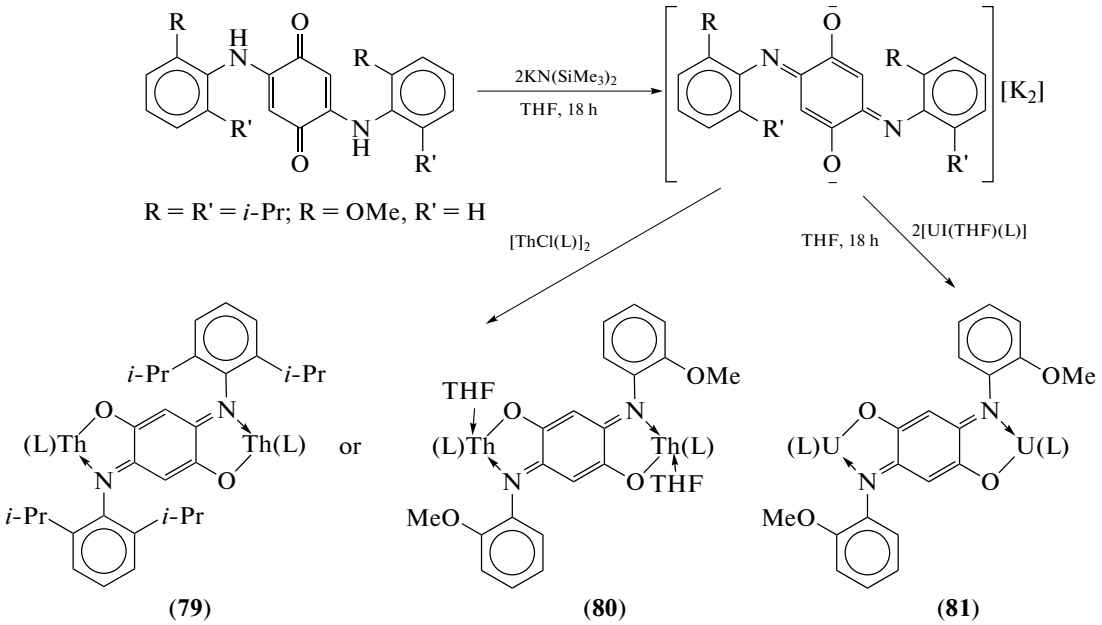

Scheme 36.

GROUP IIIa METAL COMPLEXES WITH *o*-IMINOQUINONE TYPE TRIDENTATE LIGANDS

Complexes of boron group elements. The dimethyl derivatives of Group IIIa metals containing a tridentate ONN-ligand are obtained via reactions of the enamine form of *N*-(1-(5,7-di-*tert*-butyl-2-methyl-2,3-dihydrobenzo[d]oxazol-2-yl)ethylidene)-2,6-diisopropylaniline with Me_3M (M = Al, Ga, In, Tl) (Scheme 37) [43]. Despite the presence of two alkyl groups in the metal coordination sphere, crystalline complexes **82**–**85** are stable to air oxygen and moisture; however, in solutions of **82** in various solvents, one of the methyl groups migrates from aluminum to the ligand C=N group (Scheme 37). Unlike aluminum and gallium derivatives, complexes **84** and **85** exhibit intense photoluminescence at room temperature, which makes them promising for the design of photoactive materials.

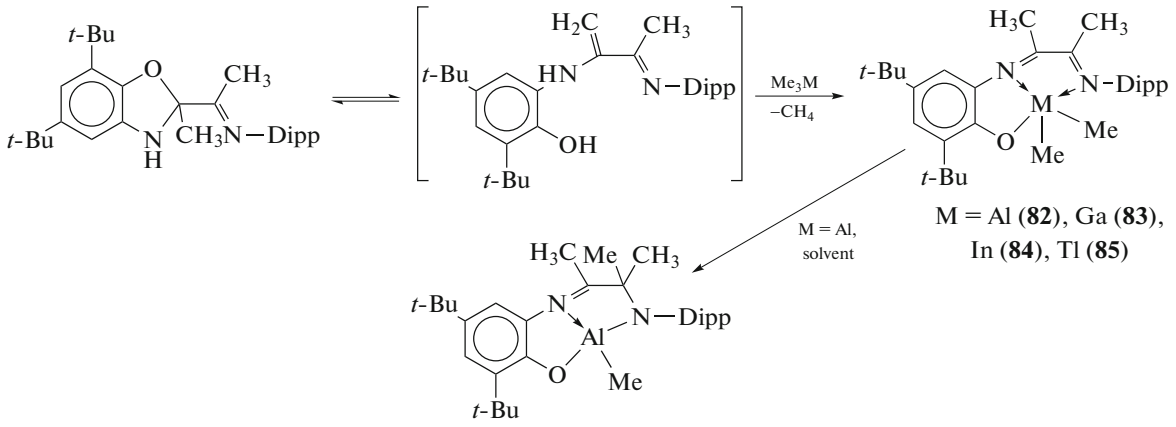

Scheme 37.

An abundant series of monomeric boronates **86** was prepared by condensation of unsymmetrical amino-bis-phenols with various arylboronic acids (Scheme 38) [44]. The boron atom in **86** has a tetrahedral environment formed via covalent bonding to oxygen atoms of the tridentate ligand and the donor-acceptor coordination of the protonated sp^3-hybridized nitrogen atom.

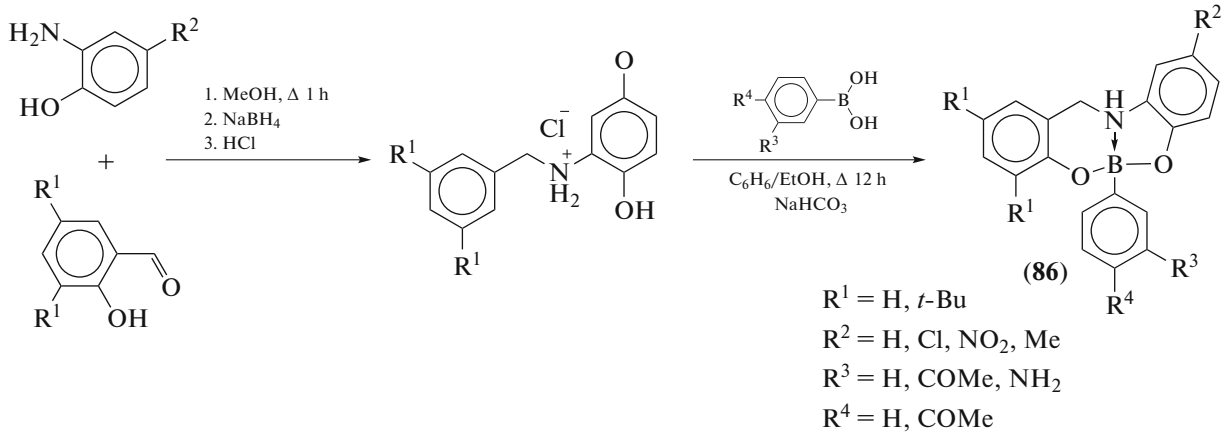

Scheme 38.

A similar coordination environment is inherent in the boron atom in compounds **87** prepared by condensation of unsubstituted bis-phenolamines and phenylboronic acid (Scheme 39) [45].

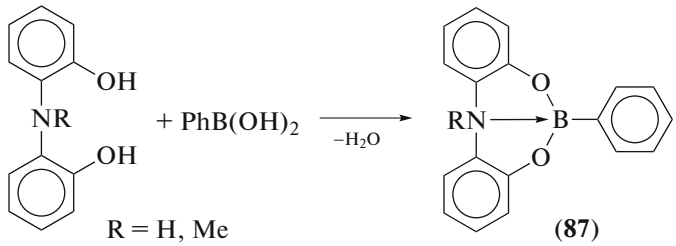

Scheme 39.

Quite a few Group III metal complexes were prepared from 3,5-di-*tert*-butyl-1,2-quinone-1-(2-hydroxy-3,5-di-*tert*-butylphenyl)imine (ONO). This tridentate ligand contains two oxygen atoms in the *ortho*-positions relative to the N atom. Being complexed with a metal, it can exist in four redox states (Scheme 40) [46]. The neutral (ONO^0) and doubly reduced (ONO^2) forms are radicals, whereas mono- (ONO^1) and trianions (ONO^3) are diamagnetic.

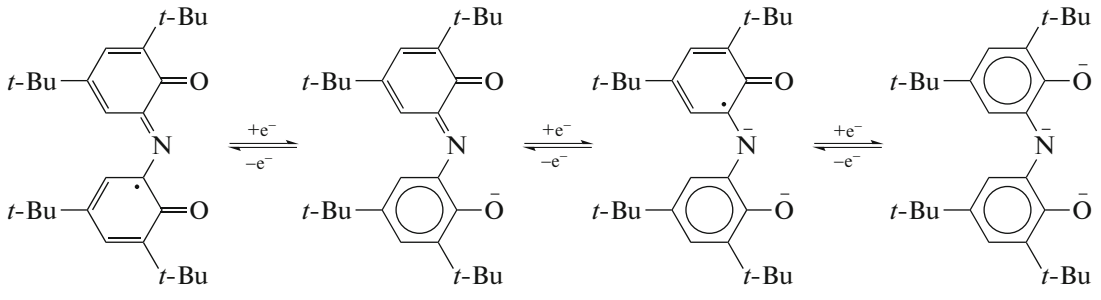

Scheme 40.

The geometry of the coordination unit in the boron complex $(ON(H)O^3)BCl$ (**88**) prepared by transmetallation reaction between BCl_3 and the zinc complex $Zn(ONO^1)_2$ [47] is similar to that of compounds **87** based on unsubstituted bis-phenolamines.

Since free ONO ligand is unstable, the major synthetic route to metal complexes based on this ligand is the template synthesis from 3,5-di-*tert*-butylcatechol ((3,5-Cat)H_2), ammonia, and salts of appropriate metals in alcohols in the presence of air oxygen. The reaction of (3,5-Cat)H_2 with aluminum and gallium trichlorides in 4 : 1 molar ratio carried out in ethanol in the presence of air oxygen gives octahedral mixed-ligand complexes $(ONO^1)(ONO^2)M^{III}$ (M = Al (**89**), Ga (**90**)) [47]. In [48], the mixed-ligand gallium derivative **90** was synthesized by electrolysis of a solution of (3,5-Cat)H_2 in liquid ammonia with a gallium anode.

Diamagnetic thallium complexes generally described as $(ONO^1)Tl(X)Ar$ (**91**) and $(ONO^1)TlAr_2$ (**92**), where X is halogen, Ar is phenyl or substituted phenyl, are also generated via template synthesis by the reaction of 3,5-di-*tert*-butyl-*o*-aminophenol with thallium(III) mono- and diaryl complexes (2 : 1) in polar solvents [49].

A series of aluminum complexes containing one ONO ligand in various oxidation states was synthesized by exchange of aluminum halides with alkali metal salts $(ON(H)O^3)M_2$ (M = Li, K) and $(ONO^1)K$ [50]. The reactions of aluminum halides with $(ON(H)O^3)M_2$ (M = Li, K) taken in 1 : 1 ratio give five-coordinate aluminum complexes **93** and **94**, in which the metal atom occurs in a trigonal bipyramidal coordination environment (Scheme 41).

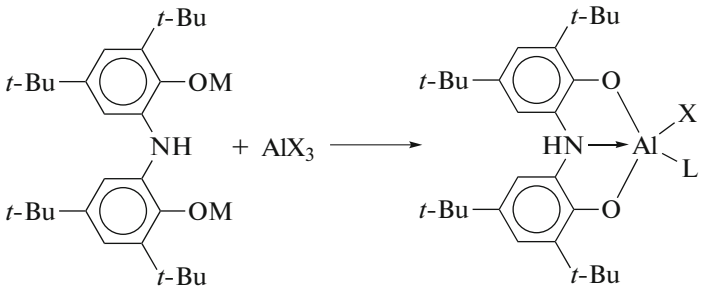

Scheme 41.

The reaction of $AlCl_3$ with the monoanionic salt $(ONO^1)K$ in the presence of stoichiometric amounts of diphenylacetylacetonate $\left(AcacPh_2^-\right)$ or 8-hydroxyquinoline ($QuinO^-$) results in the formation of octahedral aluminum complexes **95** and **96**, which can undergo single-electron reduction to monoradical derivatives **97** and **98** (Scheme 42).

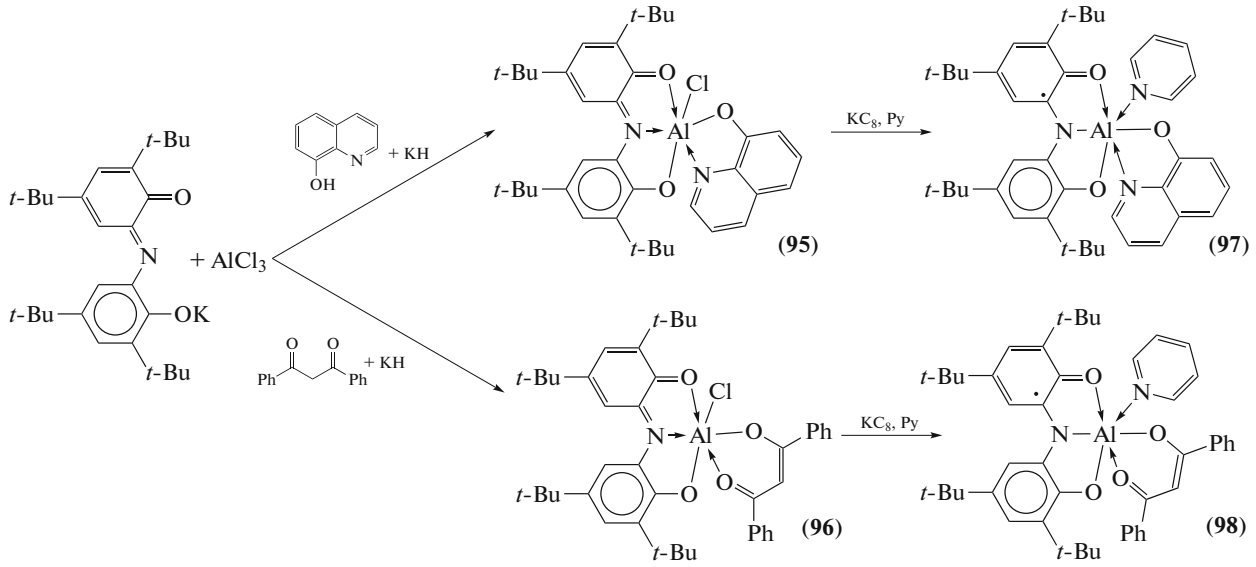

Scheme 42.

The oxidation of complex **93** with various *o*-quinones (Q) involves expulsion of HCl, resulting in the formation of aluminum complexes **99**–**101** with two redox-active ligands of different nature (Scheme 43). The electronic structures of **99**–**101** are different: in the case of less electron-withdrawing *o*-phenanthrenequinone and pyrene-4,5-dione, biradical $(ONO^2)Al(SQ)(Py)$ species are formed (SQ = is the radical anion of the corresponding *o*-quinone); meanwhile, the radical anion of the highly electron-withdrawing tetrachloro-*o*-quinone can oxidize ONO to the monoanion ONO^1 and, hence, the electronic structure of complex **99** should be considered as a combination of two forms, $(ONO^2)Al(SQ)(Py)$ and $(ONO^1)Al(Cat)(Py)$ (Cat = *o*-quinone dianion).

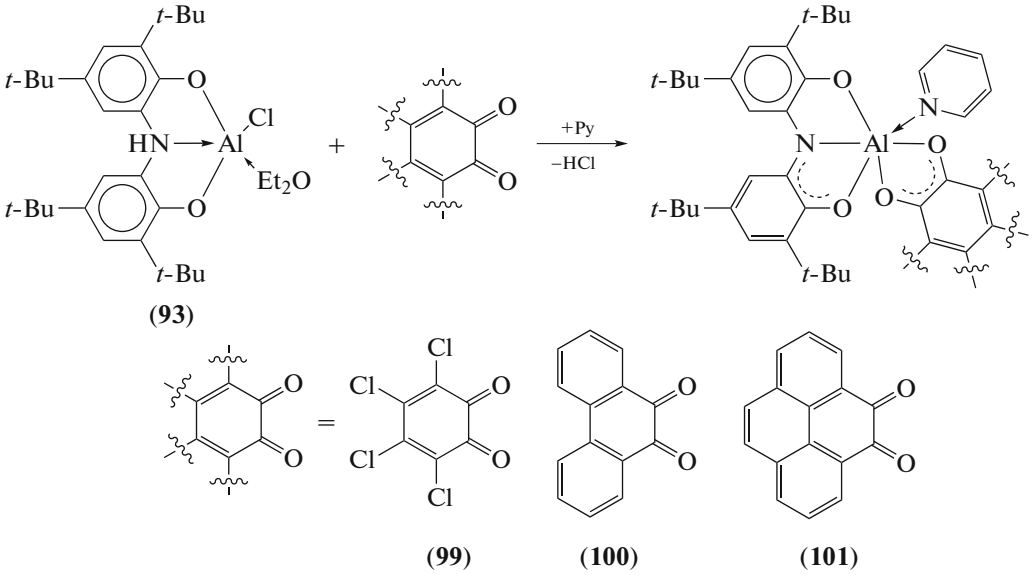

Scheme 43.

The binuclear dianionic gallium complex **102** was synthesized by the reaction of hexadentate 1,2-bis(3,5-di-*tert*-butyl-2-hydroxyphenyl)oxamine (H_4(Bbpo)) with two equivalents of gallium chloride in the presence of an ammonium salt (Scheme 44) [51]. Each gallium atom in **102** has a distorted trigonal bipyramidal environment.

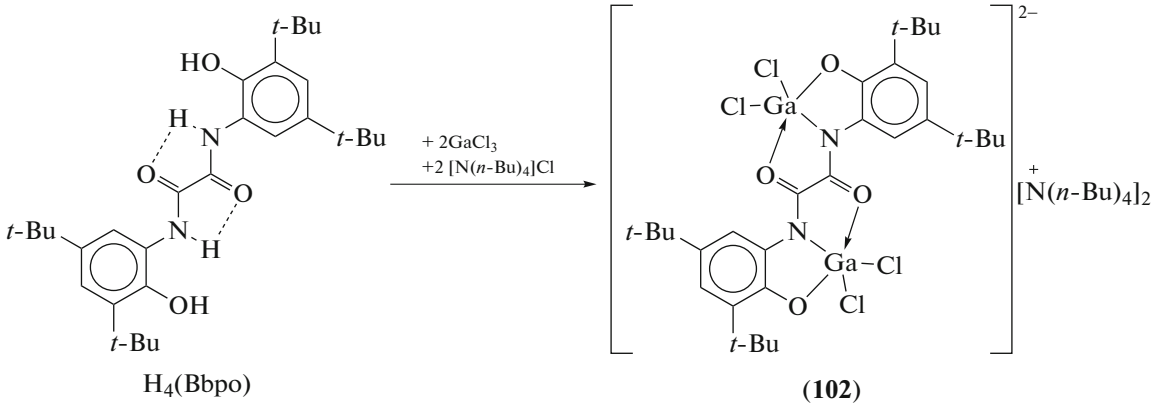

Scheme 44.

Electrochemical oxidation of the diamagnetic dianion **102** proceeds reversibly in two single-electron steps giving mono- and biradical derivatives, respectively (Scheme 45).

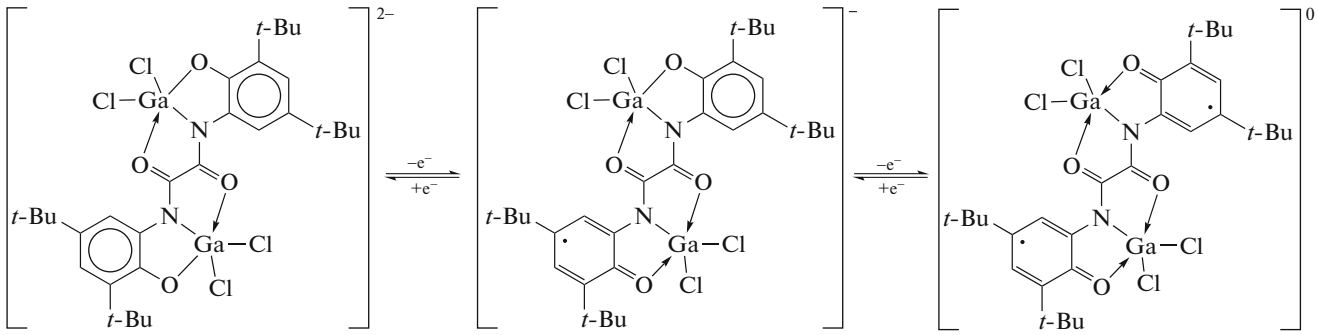

(**102**)

Scheme 45.

Rare earth metal and actinide complexes. Tris-ligand *o*-iminobenzoquinone rare earth metal complexes $(ONO^1)_3M^{III}$ (M = Sc, Y, La, Ce, Pr, Nd, Sm, Eu, Gd, Tb, Dy, Ho, Er, Tm, Yb, Lu) were prepared for the first time by template synthesis from 3,5-di-*tert*-butylcatechol and the chlorides or nitrates of the appropriate metals in the presence of ammonia in aqueous ethanol [52].

The complexes $(ONO^1)_3M^{III}$ (M = La (**103**), Sm (**104**), Yb (**105**)) can also be prepared by the reaction of bis(2-hydroxy-3,5-di-*tert*-butylphenyl)amine (ONO^3H_3) with hydrated metal chlorides in the presence of amine or by the reaction of 3,5-di-*tert*-butyl-1,2-quinone-1-(2-hydroxy-3,5-di-*tert*-butylphenyl)imine (ONO^1H) with silylamides of the same metals (3 : 1) [53]. According to X-ray diffraction data, the metal atom in $(ONO^1)_3M$ (M = La (**103**) [53], Sm (**104**) [54]) exists in the trivalent state and is coordinated to three equivalent ONO^1 ligands; the metal coordination number is nine; and the coordination polyhedron is a tricapped trigonal prism. Complexes **103** and **104** and the aluminum complex $(ONO^1)(ONO^2)Al$ (**89**) served as the basis for photovoltaic cells; the best characteristics were recorded for semiconductor devices with the photoactive layer based on the aluminum compound [53].

A series of nine-coordinate tris-chelate lanthanide(III) complexes **106** was synthesized by reactions of the reduced form of the tridentate 2,4,6,8-tetrakis(*tert*-butyl)-9-hydroxyphenoxazin-1-one ligand ($(ONO')H_3$) with the acetates $(OAc)_3Ln$ (Ln = La, Pr, Sm, Eu, Gd, Tb, Dy, Yb) (Scheme 46) [55, 56]. The coordination polyhedron of $(ONO')_3Ln$ (Ln = La, Pr, Sm, Eu, Gd, Tb, Dy), like that of $(ONO)_3Ln$ (Ln = La (**103**), Sm (**104**)), is a tricapped trigonal prism formed by six oxygen atoms and three nitrogen atoms of the deprotonated ONO' ligand.

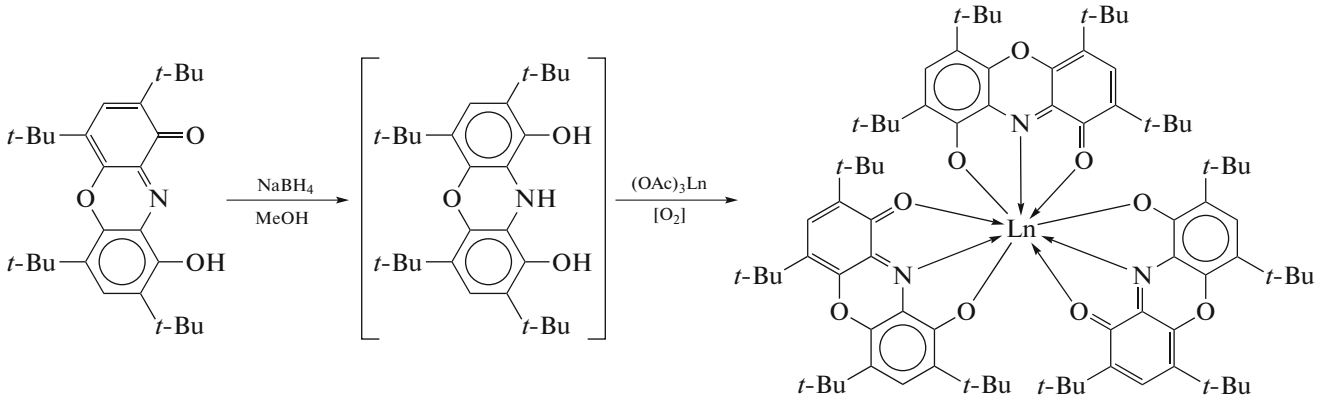

(ONO')H (ONO')H_3 $(ONO')_3Ln$ (**106**)

(Ln = La, Pr, Sm, Eu, Gd, Tb, Dy, Yb)

Scheme 46.

Uranium complex **107** containing the ONO' ligand in the above-considered monoanionic form is obtained by the reaction of (ONO')H with uranyl bis-trimethylsilylamide (Scheme 47) [57]. The possibility of preparing the complex with the most oxidized form of the ligand is provided by the use of uranium(VI) as the starting compound, which rules out the intramolecular redox process resulting in reduction of the redox-active ligand.

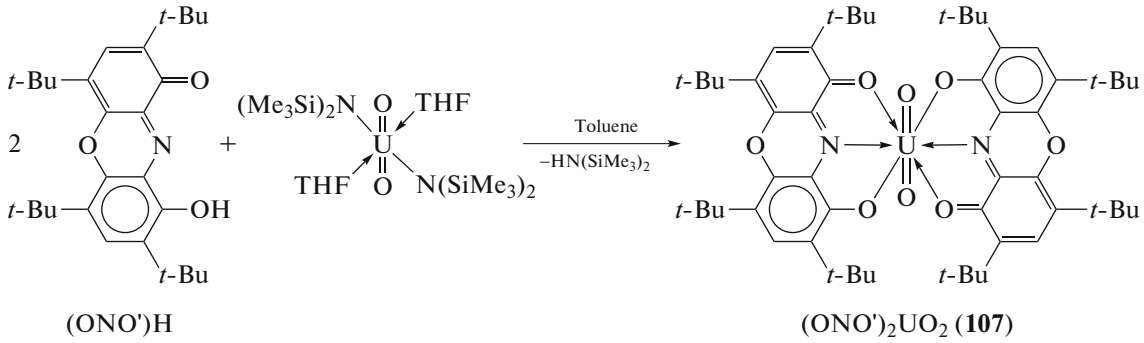

Scheme 47.

Meanwhile, the reaction of uranium(III) iodide with the monopotassium salt (ONO')K, similarly to the synthesis of *o*-iminoquinone complex **69**, is accompanied by metal-to-ligand electron transfer and gives uranium(IV) complex **108** containing a doubly reduced ligand (Scheme 48). When this reaction is conducted in the presence of an equivalent of KC_8, reduction of the redox-active ligand takes place, and the resulting complex **109** contains ONO' in the trianionic state. Compound **109** is also generated by direct reduction of **108** with potassium carbide (Scheme 48).

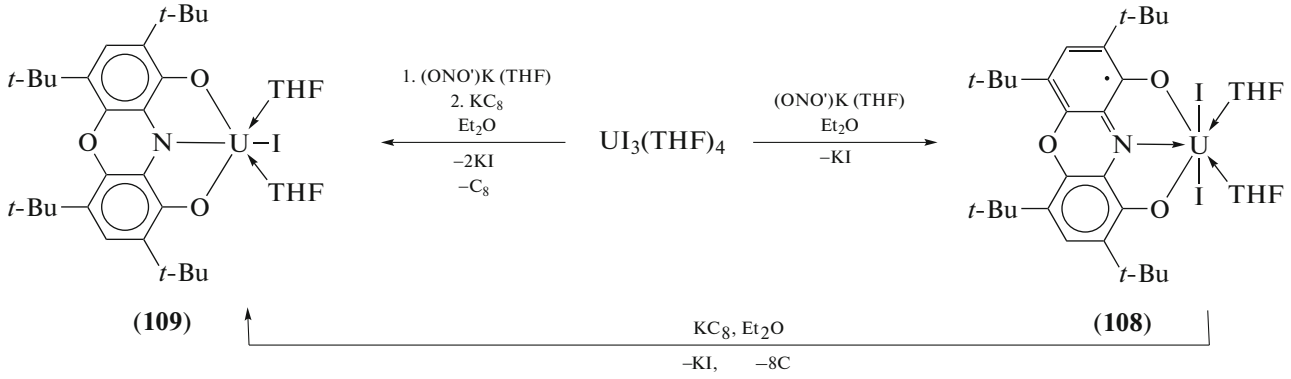

Scheme 48.

The pentamethylcyclopentadienyl analogue of **109**, $(ONO')U^{IV}(Cp^*)(THF)_2$ (**110**), was prepared by a similar pathway; the complex $(Cp^*)U^{III}I_2(THF)_3$ generated in situ from $UI_3(THF)_4$ and K(Cp*) was used as the starting uranium compound.

COMPLEXES OF GROUP III METALS WITH TETRADENTATE *o*-IMINOQUINONE TYPE LIGANDS

The chemistry of Group III metal complexes with tetradentate *o*-iminoquinone ligands is much less studied than that for silicon Group elements [14]. A series of six-coordinate aluminum complexes **111**–**114** stabilized by phosphine oxide donor ligands was synthesized by the reactions of potential tetradentate $N_2O_2^{3-}$ formazanate ligands ($Form^R$) with $Al(OiPr)_3$ in the presence of two equivalents of phosphine oxides of different nature (Scheme 49) [58]. The aluminum atom in **111**–**114** occurs in an octahedral environment formed by the O,N,N,O atoms of the formazanate ligand in equatorial positions and two phosphine oxide donors in axial positions. Complex **112** in combination with $(n\text{-}Pr)_3N$ is an electroluminescent emitter with electroluminescence maximum at 735 nm, which attests to potential use of six-coordinate formazanate aluminum complexes as functional materials.

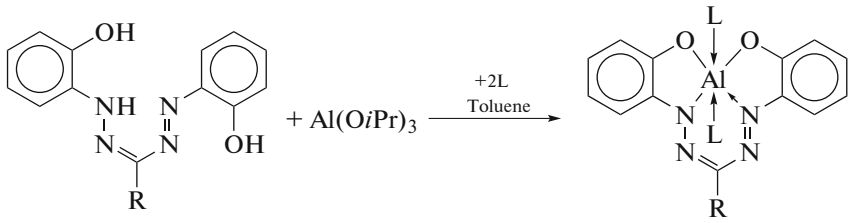

Form^R (R = Ph, CN)

(**111**) (R = Ph, L = $OPPh_3$)
(**112**) (R = CN, L = $OPPh_3$)
(**113**) (R = Ph, L = $OPBu_3$)
(**114**) (R = Ph, L = $OP(CH_2CH_2Fc)_3$)

Scheme 49.

The reaction of Form^{CN} with $BF_3 \cdot OEt_2$ in the presence of triehylamine does not lead to four-coordinate boron complex with formazanate O,N,N,O-coordination, as in the case of aluminum compounds **111**–**114**, since in this case, five-membered chelate rings that could be formed would have been too strained; instead, a mixture of sterically less crowded compounds **115**–**119** is formed during the reaction (Scheme 50) [59].

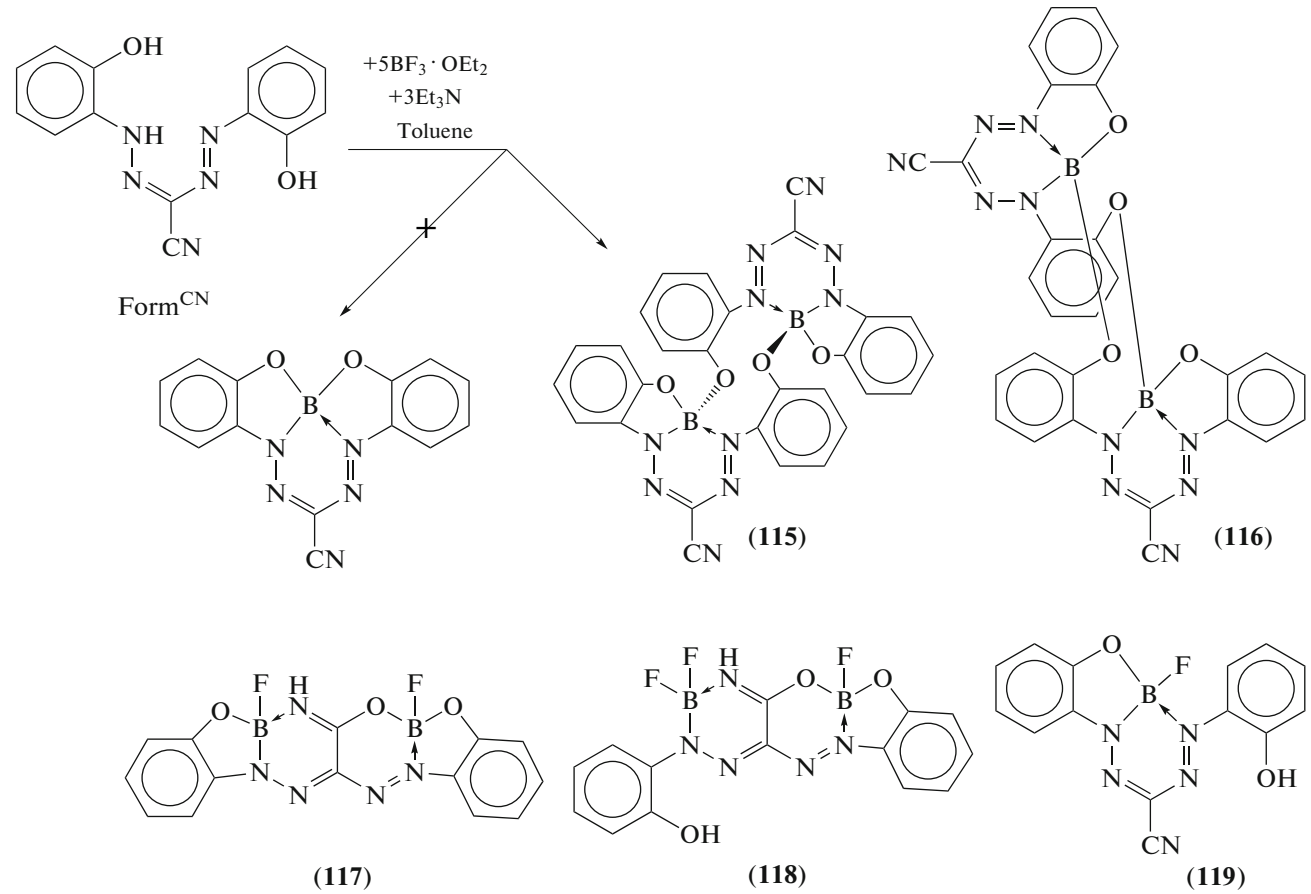

Scheme 50.

The tetradentate ONNO ligand formed upon condensation of 3,5-di-*tert*-butylcatechol and ethylenediamine reacts with one equivalent of $AlEt_3$ in THF to give the expected ethyl aluminum complex **120**, whereas addition of a non-polar solvent (pentane) to the reaction mixture is accompanied by the formation of dimer **121** (Scheme 51) [60]. The coordination geometry of each five-coordinate

metal center in **121** is a nearly perfect square pyramid with the base being formed by planar coordination of the tetradentate ONNO ligand and the apical position being occupied by the bridging nitrogen atom. Dimer **121** reacts with two equivalents of benzyl alcohol at room temperature to give alkoxide derivative **122**. Complexes **120**–**122** exhibit a high catalytic activity towards ring opening polymerization of *rac*-lactide at room temperature; furthermore, the catalyst system can be generated in situ from ONNO and $AlEt_3$ in THF after the subsequent (15 min later) addition of a benzyl alcohol–*rac*-lactide mixture (1 : 100).

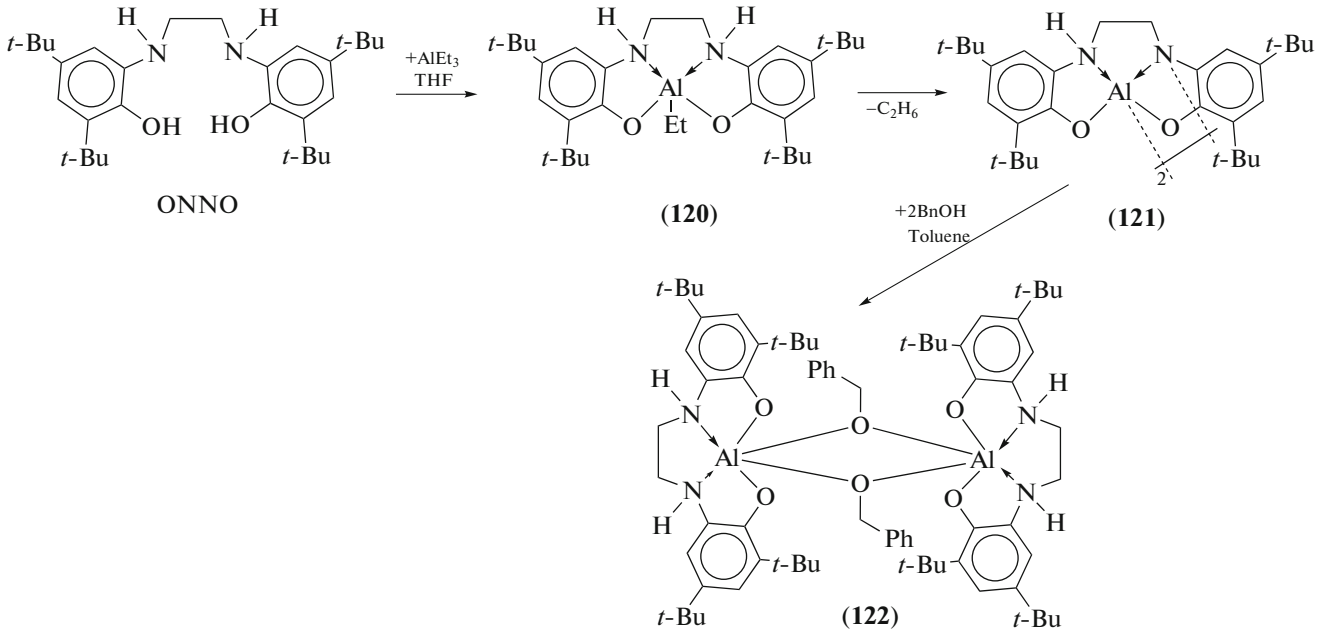

Scheme 51.

Tetradentate *N*,*N*'-bis-(iminophenol)acenaphthene (Phen-BIAN) reacts with $UO_2(OAc)_2$ in ethanol to give diamagnetic oxide-bridged dimer **123** containing two uranyl metal centers and Phen-BIAN coordinated in the tetradentate fashion; as a result, each UO_2 center occurs in a pentagonal-bipyramidal coordination environment (Scheme 52) [61]. The electrochemical reduction of the complex demonstrates a wide range of uranium oxidation states that can be attained via the formation of U(VI)/U(V) and U(V)/U(IV) mixed-valence derivatives in solution.

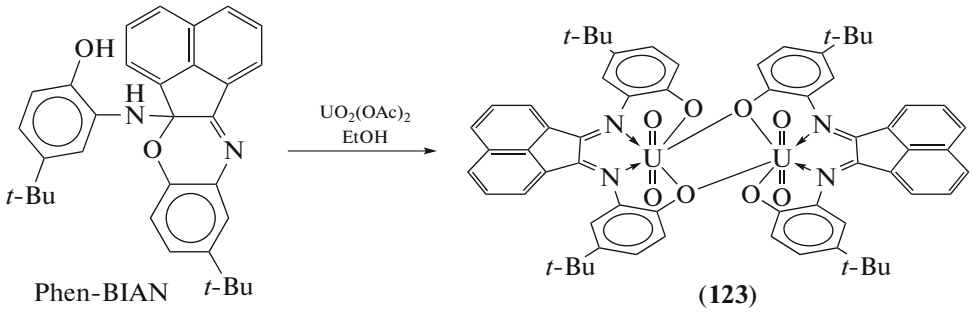

Scheme 52.

In conclusion, it is noteworthy that the field of chemistry addressing metal complexes with various redox-active ligands has been intensively developed in recent years and is covering more and more compounds. New types of organic ligands capable of changing the oxidation state within a metal coordination sphere are synthesized and known redox-active systems are deliberately modified. The *o*-iminoquinone ligands possess a great potential for such a modification, which is attained by introducing various

functional substituents into the nitrogen-containing moiety [62–74]. One more promising trend in this area is reflected by the first studies of *o*-iminoquinone complexes of rare earth elements and actinides [37–42, 53, 55–57, 61].

FUNDING

The study was performed within a state assignment.

CONFLICT OF INTEREST

The authors declare that they have no conflict of interest.

REFERENCES

1. Tezgerevska, T., Alley, K.G., and Boskovic, C., *Coord. Chem. Rev.*, 2014, vol. 268, p. 23.
2. Broere, D.L.J., Plessius, R., and van der Vlugt, J.I., *Chem. Soc. Rev.*, 2015, vol. 44, p. 6886.
3. Jacquet, J., Cheaib, K., Ren, Y., et al., *Chem.-Eur. J.*, 2017, vol. 23, p. 1530.
4. Kaim, W. and Paretzki, A., *Coord. Chem. Rev.*, 2017, vol. 344, p. 345.
5. Abakumov, G.A., Piskunov, A.V., Cherkasov, V.K., et al., *Russ. Chem. Rev.*, 2018, vol. 87, p. 393.
6. Van der Vlugt, J.I., *Chem.-Eur. J.*, 2019, vol. 25, p. 2651.
7. Broere, D.L.J., van Leest, N.P., de Bruin, B., et al., *Inorg. Chem.*, 2016, vol. 55, p. 8603.
8. Bagh, B., Broere, D.L.J., Sinha, V., et al., *J. Am. Chem. Soc.*, 2017, vol. 139, p. 5117.
9. Paul, G.C., Ghorai, S., and Mukherjee, C., *Chem. Commun.*, 2017, vol. 53, p. 8022.
10. Leconte, N., d'Hardemare, A.M., Philouze, C., and Thomas, F., *Chem. Commun.*, 2018, vol. 54, p. 8241.
11. Yakub, A.M., Moskalev, M.V., Bazyakina, N.L., and Fedushkin, I.L., *Russ. Chem. Bull.*, 2018, vol. 67, p. 473.
12. Zhang, W., Dodonov, V.A., Chen, W., et al., *Chem.-Eur. J.*, 2018, vol. 24, p. 14994.
13. Dodonov, V.A., Chen, W., Zhao, Y., et al., *Chem.-Eur. J.*, 2019, vol. 25, p. 8259.
14. Chegerev, M.G., Piskunov, A.V., *Russ. J. Coord. Chem.*, 2018, vol. 44, p. 258. https://doi.org/10.1134/S1070328418040036).
15. Kimmich, B.F.M., Landis, C.R., and Powell, D.R., *Organometallics*, 1996, vol. 15, p. 4141.
16. Barba, V., Rodriguez, A., Ochoa, M.E., et al., *Inorg. Chim. Acta*, 2004, vol. 357, p. 2593.
17. Alibadi, M.A.M., Batsanov, A.S., Bramham, G., et al., *Dalton Trans.*, 2009, p. 5348.
18. Gracey, G.D., Rettig, S.J., Storr, A., and Trotter, J., *Can. J. Chem.*, 1987, vol. 65, p. 2469.
19. Piskunov, A.V., Maleeva, A.V., Mescheryakova, I.N., and Fukin, G.K., *Eur. J. Inorg. Chem.,* 2012, vol. 2012, p. 4318.
20. Piskunov, A.V., Mescheryakova, I.N., Ershova, I.V., and Fukin, G.K., *Inorg. Chem. Commun.*, 2012, vol. 24, p. 227.
21. Piskunov, A.V., Ershova, I.V., Fukin, G.K., and Shavyrin, A.S., *Inorg. Chem. Commun.*, 2013, vol. 38, p. 127.
22. Piskunov, A.V., Mescheryakova, I.N., Bogomyakov, A.S., et al., *Inorg. Chem. Commun.*, 2009, vol. 12, p. 1067.
23. Piskunov, A.V., Mescheryakova, I.N., Fukin, G.K., et al., *New J. Chem.*, 2010, vol. 34, p. 1746.
24. Piskunov, A.V., Meshcheryakova, I.N., Fukin, G.K., et al., *Dalton Trans.*, 2013, vol. 42, p. 10533.
25. Piskunov, A.V., Ershova, I.V., Fukin, G.K., *Russ. Chem. Bull.*, 2014., vol. 63, p. 916.
26. Piskunov, A.V., Meshcheryakova, I.N., Ershova, I.V., et al., *RSC Adv.*, 2014, vol. 4, p. 42494.
27. Ershova, I.V., Bogomyakov, A.S., Fukin, G.K., and Piskunov, A.V., *Eur. J. Inorg. Chem.,* 2019, vol. 2019, p. 938.
28. Piskunov, A.V., Ershova, I.V., Bogomyakov, A.S., et al., *Inorg. Chem.*, 2015, vol. 54, p. 6090.
29. Piskunov, A.V., Ershova, I.V., Bogomyakov, A.S., and Fukin, G.K., *Inorg. Chem. Commun.*, 2016, vol. 66, p. 94.
30. Chaudhuri, P., Wagner, R., Pieper, U., et al., *Dalton Trans.*, 2008, p. 1286.
31. Chaudhuri, P., Bill, E., Wagner, R., et al., *Inorg. Chem.*, 2008, vol. 47, p. 5549.
32. Bamford, K.L., Longobardi, L.E., Liu, L., et al., *Dalton Trans.*, 2017, vol. 46, p. 5308.
33. Gao, B., Su, Q., Gao, W., and Mu, Y., *Acta Crystallogr., Sect. E: Struct. Rep. Online,* 2011, vol. 67, p. m1374.
34. Razborov, D.A., Lukoyanov, A.N., Makarov, V.M., et al., *Russ. Chem. Bull.*, 2015, vol. 64, p. 2377.
35. Razborov, D.A., Lukoyanov, A.N., Moskalev, M.V., et al., *Russ. J. Coord. Chem.,* 2018, vol. 44, p. 380. https://doi.org/10.1134/S1070328418060040
36. Poddel'sky, A.I., Abakumov, G.A., Bubnov, M.P., et al., *Russ. Chem. Bull. Int. Ed.*, 2004, vol. 53, p. 1189.
37. Bochkarev, M.N., Fagin, A.A., Druzhkov, N.O., et al., *J. Organomet. Chem.*, 2010, vol. 695, p. 2774.
38. Klementyeva, S.V., Lukoyanov, A.N., Afonin, M.Yu., et al., *Dalton Trans.*, 2019, vol. 48, p. 3338.
39. Coughlin, E.J., Zeller, M., and Bart, S.C., *Angew. Chem., Int. Ed. Engl.*, 2017, vol. 56, p. 12142.
40. Matson, E.M., Franke, S.M., Anderson, N.H., et al., *Organometallics*, 2014, vol. 33, p. 1964.
41. Matson, E.M., Opperwall, S.R., Fanwick, P.E., and Bart, S.C., *Inorg. Chem.*, 2013, vol. 52, p. 7295.
42. Hohloch, S., Pankhurst, J.R., Jaekel, E.E., et al., *Dalton Trans.*, 2017, vol. 46, p. 11615.
43. Egorova, E.N., Druzhkov, N.O., Shavyrin, A.S., et al., *RSC Adv.*, 2015, vol. 5, p. 19362.
44. Abreu, A., Alas, S.J., Beltran, H.I., et al., *J. Organomet. Chem.*, 2006, vol. 691, p. 337.
45. Farfan, N., Joseph-Nathan, P., Chiquete, L.M., and Contreras, R., *J. Organomet. Chem.*, 1988, vol. 348, p. 149.
46. Chaudhuri, P., Hess, M., Hildenbrand, K., et al., *Inorg. Chem.*, 1999, vol. 38, p. 2781.
47. Camacho-Camacho, C., Merino, G., Martinez-Martinez, F.J., et al., *Eur. J. Inorg. Chem.,* 1999, p. 1021.

48. Brown, M.A., Castro, J.A., McGarvey, B.R., and Tuck, D.G., *Can. J. Chem.*, 1999, vol. 77, p. 502.
49. Stegmann, H.B., Ulmschneider, K.B., and Scheffler, K., *J. Organomet. Chem.*, 1974, vol. 72, p. 41.
50. Szigethy, G. and Heyduk, A.F., *Dalton Trans.*, 2012, vol. 41, p. 8144.
51. Beckmann, U., Bill, E., Weyhermuller, T., and Wieghardt, K., *Eur. J. Inorg. Chem.,* 2003, vol. 2003, p. 1768.
52. Lyubchenko, S.N., Kogan, V.A., and Olekhnovich, L.P., *Russ. J. Coord. Chem.,* 1996, vol. 22, p. 534.
53. Maleev, A.A., Trofimova, O.Yu., Pushkarev, A.P., et al., *Nanotechnol. Russia,* 2015, vol. 10. p. 613.
54. Furmanova, N.G., Lyubchenko, S.N., Kogan, V.A., and Olekhovich, L.P., *Crystallogr. Rep.*, 2000, vol. 45, p. 439.
55. Ivakhnenko, E.P., Simakov, V.I., Knyazev, P.A., et al., *Mendeleev Commun.*, 2016, vol. 26, p. 49.
56. Ivakhnenko, E.P., Romanenko, G.V., Simakov, V.I., et al., *Inorg. Chim. Acta*, 2017, vol. 458, p. 116.
57. Pattenaude, S.A., Kuehner, C.S., Dorfner, W.L., et al., *Inorg. Chem.*, 2015, vol. 54, p. 6520.
58. Maar, R.R., Kenaree, A.R., Zhang, R., et al., *Inorg. Chem.*, 2017, vol. 56, p. 12436.
59. Barbon, S.M., Staroverov, V.N., and Gilroy, J.B., *Angew. Chem., Int. Ed. Engl.*, 2017, vol. 56, p. 8173.
60. Gesslbauer, S., Cheek, H., White, A.J.P., and Romain, C., *Dalton Trans.*, 2018, vol. 47, p. 10410.
61. Niklas, J.E., Farnum, B.H., Gorden, J.D., and Gorden, A.E.V., *Organometallics*, 2017, vol. 36, p. 4626.
62. Broere, D.L.J., Metz, L.L., de Bruin, B., et al., *Angew. Chem., Int. Ed. Engl.*, 2015, vol. 54, p. 1516.
63. Paretzki, A., Hübner, R., Ye, S., et al., J. Mater. Chem., 2015, vol. 3, p. 4801.
64. Piskunov, A.V., Ershova, I.V., Gulenova, M.V., et al., *Russ. Chem. Bull.*, 2015, vol. 64, p. 642.
65. Ali, A., Dhar, D., Barman, S.K., et al., *Inorg. Chem.*, 2016, vol. 55, p. 5759.
66. Broere, D.L.J., Plessius, R., Tory, J., et al., *Chem.-Eur. J.*, 2016, vol. 22, p. 13965.
67. Maity, S., Kundu, S., Bera, S., et al., *Eur. J. Inorg. Chem.,* 2016, vol. 2016, p. 3691.
68. Bubrin, M., Paretzki, A., Hübner, R., et al., Z. Anorg. Allg. Chem., 2017, vol. 643, p. 1621.
69. Maity, S., Kundu, S., Mondal, S., et al., *Inorg. Chem.*, 2017, vol. 56, p. 3363.
70. Paul, G.C., Banerjee, S., and Mukherjee, C., *Inorg. Chem.*, 2017, vol. 56, p. 729.
71. Safaei, E., Bahrami, H., Wojtczak, A., et al., *Polyhedron*, 2017, vol. 122, p. 219.
72. Piskunov, A.V., Pashanova, K.I., Bogomyakov, A.S., et al., *Dalton Trans.*, 2018, vol. 47, p. 15049.
73. Ershova, I.V., Smolyaninov, I.V., Bogomyakov, A.S., et al., *Dalton Trans.*, 2019, vol. 48, p. 10723.
74. Piskunov A.V., Pashanova K.I., Ershova I.V., et al., *Izv. AN. Ser. Khim*. 2019, no. 4, pp. 757.

Translated by Z. Svitanko